

Accelerating Large Batch Training via Gradient Signal to Noise Ratio (GSNR)

Guo-qing Jiang*

Meituan Group

jianggq@pku.edu.cn

Jinlong Liu

Individual

ljlwykqh@126.com

Zixiang Ding

Meituan Group

dingzixiang@meituan.com

Lin Guo

Meituan Group

guolin08@meituan.com

Wei Lin

Individual

lwsaviola@163.com

Abstract

As models for nature language processing (NLP), computer vision (CV) and recommendation systems (RS) require surging computation, a large number of GPUs/TPUs are paralleled as a large batch (LB) to improve training throughput. However, training such LB tasks often meets large generalization gap and downgrades final precision, which limits enlarging the batch size. In this work, we develop the variance reduced gradient descent technique (VRGD) based on the gradient signal to noise ratio (GSNR) and apply it onto popular optimizers such as SGD/Adam/LARS/LAMB. We carry out a theoretical analysis of convergence rate to explain its fast training dynamics, and a generalization analysis to demonstrate its smaller generalization gap on LB training. Comprehensive experiments demonstrate that VRGD can accelerate training ($1 \sim 2\times$), narrow generalization gap and improve final accuracy. We push the batch size limit of BERT pretraining up to 128k/64k and DLRM to 512k without noticeable accuracy loss. We improve ImageNet Top-1 accuracy at 96k by 0.52pp than LARS. The generalization gap of BERT and ImageNet training is significantly reduce by over 65%.

1 Introduction

Recent machine learning models have grown wider and deeper in their architectures (e.g., GPT-3 [Floridi and Chiriatti, 2020], M6 [Lin *et al.*, 2021], Switch Transformer [Fedus *et al.*, 2021]). Training complex models may consume more training data to converge, which needs a surge in computing capacity and efficiency. However, hardware improvement can not keep pace with the expansion of model calculations [Bommasani *et al.*, 2021].

Several techniques to speed up training are proposed. For example, training with LB can notably improve throughput [You *et al.*, 2017b; Hoffer *et al.*, 2019]. You *et al.* [2020] successfully train BERT using 1024 TPUs and a LB (64k) within 76 minutes. It demonstrates the efficiency of GPUs/TPUs in large scale parallel tasks. Small batch (SB) is not able to fully utilize those powerful GPUs/TPUs.

However, the literatures point out that training with LB may lead to generalization gap. Keskar *et al.* [2017] analyze the LB training and finds that it can be easily trapped into the area with strong

*Corresponding author

generalization gap. Hoffer *et al.* [2017] indicate that the generalization gap can be attributed to the fewer update steps in LB training compared with SB when using identical epochs. Dai and Zhu [2018] theoretically demonstrate that training with more steps or expanding the learning rate to batch size ratio helps to converge to a flatter local minimum.

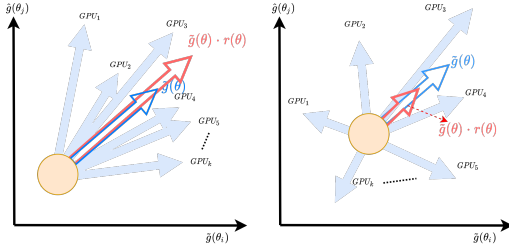


Figure 1: Schematic of VRGD’s mechanism: updating parameters with larger GSNR (left panel) and smaller GSNR (right panel).

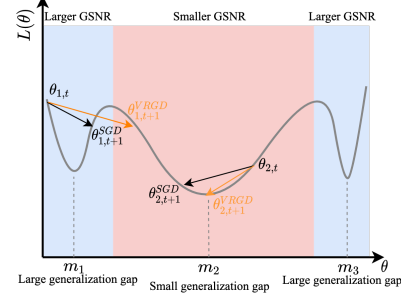


Figure 2: Larger GSNR helps the weights to escape from the large generalization gap area, while smaller GSNR attracts the weights to stay in small generalization gap area.

Liu *et al.* [2020a] point out that updating those weights with small GSNR leads to generalization gap (Fig.1). Inspired by the widely used LARS/LAMB [You *et al.*, 2017a, 2020] who use learning rate scaling policy, we try to update those weights with large GSNR with larger learning rate and vice visa (Fig.2), which may help reduce the generalization gap. This **element-wise adaptive** technique is called variance reduced gradient descent technique (VRGD).

Our main contributions are listed below:

- We carry out theoretical derivations of convergence rate and generalization analysis to explain why VRGD can accelerate LB training and achieve dramatically smaller generalization gap.
- We perform comprehensive LB experiments and find that VRGD can accelerate training ($1 \sim 2\times$), narrow the generalization gap and improve final precision than previous SOTA (e.g., LAMB, LARS).
- We push the batch size limit of BERT pretraining up to 128k/64k and DLRM to 512k without noticeable accuracy loss. We improve ImageNet Top-1 accuracy at 96k by 0.52pp than LARS. The generalization gap of BERT and ImageNet training is significantly reduce by over 65%.

2 Related Work

2.1 Large Batch Training

Several techniques are proposed to improve the optimization and generalization ability in LB training. Goyal *et al.* [2017] propose a linear scaling rule on learning rate (LR) to achieve the same accuracy as SB and push the batch size limit of ImageNet to 8k. EXTRAP-SGD uses the extra-gradient to stabilize the optimization trajectory and smooth training [Lin *et al.*, 2020]. SWAP quickly trains the model with LB in the first stage and refines it by averaging the weights of multiple SB models in the second stage [Gupta *et al.*, 2020]. Batch Augmentation replicates multiple instances with the same batch size to improve generalization [Hoffer *et al.*, 2019]. The batch size of the experiments in EXTRAP-SGD/SWAP/Batch-Augmentation are less than 8k and are not compared in our experiments.

DecentLaM removes the growing momentum-incurred bias observed in DmSGD and pushes ImageNet to 32k [Yuan *et al.*, 2021]. Layer-wise LR’s adjustment optimizers such as LARS [You *et al.*, 2017a], complete layer-wise adaptive rate scaling (CLARS, Huo *et al.* [2021]), LAMB [You *et al.*, 2020] successfully improve the batch size up to 64k both for ImageNet and BERT pretraining without accuracy loss. Recently, the concurrent adversarial learning (ConAdv) method pushes the

batch size limit of ImageNet training up to 96k [Liu *et al.*, 2021]. LANS replaces the layer-wise LR adjustment in LAMB with block-wise style [Zheng *et al.*, 2020] and also pushes BERT training up to 96k. Adam adds those gradients after scaling with proper scalars and even pushes the batch size limit of BERT up to 128k/32k [Maleki *et al.*, 2021].

2.2 Gradient Variance and GSNR

Unlike gradient mean, which is widely used in optimizers, gradient variance and its successor GSNR are less used. But gradient variance is frequently discussed in generalization gap. Johnson and Zhang [2013a] propose the stochastic variance reduced gradient (SVRG) with the explicit gradient variance reduction method. Other variants of SVRG like SRVR-NPG, SVRPG and Control Variate methods are also proposed to reduce the gradient variance during training [Liu *et al.*, 2020b; Wang *et al.*, 2013; Papini *et al.*, 2018; Miller *et al.*, 2017]. Rainforth *et al.* [2018] use GSNR to analyze the variational bounds in variational auto-encoder (VAE). McCandlish *et al.* [2018] use GSNR to predict the useful upper bound of batch size. Smith *et al.* [2018]; Devarakonda *et al.* [2017] adaptively increase the batch size during training to achieve acceleration without accuracy loss. Liu *et al.* [2020a] theoretically derive a quantitative relationship between GSNR and generalization gap and prove that larger GSNR leads to better generalization performance. Therefore, gradient variance and GSNR are potentially useful to train deep neural networks.

3 Preliminaries

3.1 GSNR

Given a data distribution $\mathcal{Z} = \mathcal{X} \times \mathcal{Y}$, a model $\hat{y} = f(x, \theta)$ parameterized by θ and the loss function L . The parameters' gradient w.r.t. sample (x_i, y_i) can be written as (Refer to all "notations" in the Appendix.C):

$$\mathbf{g}_i(\theta) := \frac{\partial L(y_i, f(x_i, \theta))}{\partial \theta} \quad (1)$$

Then j -th parameter' (θ_j) gradient computed using (x_i, y_i) is $\mathbf{g}_i(\theta_j)$. Here we use i to index the data samples and j to index the parameters of θ . We denote the sample-wise gradient mean as $\bar{\mathbf{g}}(\theta) = \mathbb{E}_{(x,y) \sim \mathcal{Z}}(\mathbf{g}(x, y, \theta))$ and variance of $\mathbf{g}_i(\theta)$ as $\rho^2(\theta) = \text{Var}_{(x,y) \sim \mathcal{Z}}(\mathbf{g}(x, y, \theta))$. The GSNR for each model parameter θ_j is defined as:

$$r(\theta_j) := \frac{\tilde{\mathbf{g}}^2(\theta_j)}{\rho^2(\theta_j)} \quad (2)$$

Intuitively, GSNR measures the consistency of the gradient direction of each parameter across a batch of data samples. The gradient space of the parameters tends to converge in the same direction when the GSNR is large, but diverge if the GSNR is small (Figure.1).

3.2 GSNR and Generalization Gap

Consider a training set $D = \{(x_1, y_1), \dots, (x_n, y_n)\} \sim \mathcal{Z}^{(n)}$, where n samples come from \mathcal{Z} , and a test set of dataset size (n') from $\mathcal{Z}'^{(n')}$ denoted by $D' = \{(x'_1, y'_1), \dots, (x'_{n'}, y'_{n'})\} \sim \mathcal{Z}'^{(n')}$. The empirical training and test losses can be denoted as:

$$L[D] = \frac{1}{n} \sum_{i=1}^n L(y_i, f(x_i, \theta)); \quad L[D'] = \frac{1}{n'} \sum_{i=1}^{n'} L(y'_i, f(x'_i, \theta)) \quad (3)$$

respectively. Then the empirical generalization gap is given by $L[D'] - L[D]$. Both the training loss $L[D]$ and the test loss $L[D']$ would decrease after one training step and can be denoted as $\Delta L[D]$ and $\Delta L[D']$ respectively. The ratio between the expectations of $\Delta L[D]$ and $\Delta L[D']$ for one training step can be denoted as:

$$\mathbf{R}(\mathcal{Z}, n) := \frac{E_{D, D' \sim \mathcal{Z}^n}(\Delta L[D'])}{E_{D \sim \mathcal{Z}^n}(\Delta L[D])} \quad (4)$$

Assumption 1 (Non-overfitting limit approximation of Liu *et al.* [2020a]). *The parameters' gradient over the training set and test set i.e., $\mathbf{g}_D(\theta)$ and $\mathbf{g}_{D'}(\theta)$ obey the same distribution.*

Based on Assumption 1 and using a small learning rate $\lambda \rightarrow 0$, Liu *et al.* [2020a] derive the relationship between the one-step generalization ratio (eq.4) and GSNR:

$$\mathbf{R}(\mathcal{Z}, n) = 1 - \frac{1}{n} \sum_j W_j \frac{1}{r_j + \frac{1}{n}}, \text{ where } W_j := \frac{E_{D \sim \mathcal{Z}^n}(\Delta L_j[D])}{E_{D \sim \mathcal{Z}^n}(\Delta L[D])} \text{ with } \sum_j W_j = 1 \quad (5)$$

where $\Delta L_j[D]$ is the training loss reduction caused by updating θ_j . A more *detailed mathematical derivation* can be found in Liu *et al.* [2020a]. This relationship (eq.5) demonstrates that GSNR (r_j) plays a crucial role in determining the generalization performance of the model. Updating the model parameters with smaller GSNR leads to generalization gap growth. Also note that we have $\mathbf{R}(\mathcal{Z}, n) \rightarrow 1$ when $n \rightarrow \infty$, which means that training with a larger dataset helps generalization.

4 Proposed Algorithms

In this section, we propose VRGD with their general updating rules (taking VR-SGD as an example in Algorithm.1). The SGD is shown in Appendix.D for comparison.

Algorithm 1: VR – SGD

Input: require device number $k \geq 2$

Input: $B = \text{GlobalBatchSize}/k$

Input: $\gamma = 0.1$

```

1 while  $\theta_t$  not converged do
    for device  $d = 1$  to  $k$  do
         $\tilde{\mathbf{g}}_d(\theta_t) \leftarrow \frac{1}{B} \sum_{i=1}^B \nabla_{\theta} L(y_i, f(x_i, \theta_{t-1}))$  (Get gradient on each GPU/TPU)
         $\tilde{\mathbf{g}}_d^2(\theta_t) \leftarrow \tilde{\mathbf{g}}_d(\theta_t) \otimes \tilde{\mathbf{g}}_d(\theta_t)$  (Element-wise multiply, so as square terms below)
     $\tilde{\mathbf{g}}(\theta_t) \leftarrow \frac{1}{k} \sum_{d=1}^k \tilde{\mathbf{g}}_d(\theta_t)$  (Reduce gradient over all devices)
     $\sigma_t^2 \leftarrow \frac{1}{k} \sum_{d=1}^k \tilde{\mathbf{g}}_d^2(\theta_t) - \tilde{\mathbf{g}}^2(\theta_t)$  (Compute gradient variance)
     $r(\theta_t) \leftarrow \frac{\tilde{\mathbf{g}}^2(\theta_t)}{\sigma_t^2}$  (Compute GSNR)
    for layer  $l = 0$  to  $h$  do
         $r(\theta_t^{(l)}) \leftarrow \frac{r(\theta_t^{(l)})}{\frac{1}{J} \sum_{j=1}^J r(\theta_{t,j}^{(l)})}$  (Normalize GSNR so that  $\overline{r(\theta_t^{(l)})} = 1$ )
         $r(\theta_t^{(l)}) \leftarrow \begin{cases} \gamma, & \text{if } r(\theta_t^{(l)}) < \gamma \\ 1, & \text{if } r(\theta_t^{(l)}) > 1 \end{cases}$  (Confine the max/min ratio within  $\frac{1}{\gamma}$ )
     $\theta_t \leftarrow \theta_{t-1} - \lambda \cdot r(\theta_t) \cdot \tilde{\mathbf{g}}(\theta_t)$  (Update weights)

```

4.1 VR-SGD's Updating Rules

Consider the simple updating rule for SGD as follows:

$$\theta_t = \theta_{t-1} - \lambda \cdot \tilde{\mathbf{g}}(\theta_t) \quad (6)$$

where λ is the learning rate. Previous section demonstrates that updating the weights with larger GSNR confines the model's generalization gap growth during training. Therefore, GSNR can be used in the optimizer for better generalization. In the mathematical derivation of GSNR's role on the generalization gap, all sample-wise gradients for the entire dataset are used to compute the gradient variance, which is less efficient. However, in the LB training, where each batch is large enough to accurately estimate the gradient variance, we replace the entire dataset with a LB and the sample-wise with device-wise gradient computation. Gradients on each GPU/TPU device can be synchronized using Ring-AllReduce, thus perfectly avoiding the inefficiency of gradient variance computation. The simplified gradient variance computation is as follows:

$$\sigma_t^2 = \frac{1}{k} \sum_{d=1}^k \tilde{\mathbf{g}}_d^2(\theta_t) - \tilde{\mathbf{g}}^2(\theta_t) \quad (7)$$

where k devices are used, each of which computes $1/k$ part of the gradient $\tilde{\mathbf{g}}_d(\theta_t)$, the same as what data parallel does. The GSNR can then be easily calculated based on eq.2 ($\rho^2(\theta_j)$ is replaced by σ_j^2). The mean values of GSNR are removed at each layer before applying gradient to the parameters. This normalization of GSNR ensures that the global averaged GSNR remains at 1.0:

$$r(\theta_t^{(l)}) = \frac{r(\theta_t^{(l)})}{\frac{1}{J} \sum_{j=1}^J r(\theta_{t,j}^{(l)})} \quad (8)$$

where l^{th} layer contains J parameters. We constrain the *max/min* of GSNR within $1/\gamma$ so that those neurons with very small GSNR remain active:

$$r(\theta_t^{(l)}) = \begin{cases} \gamma, & \text{if } r(\theta_t^{(l)}) < \gamma \\ 1, & \text{if } r(\theta_t^{(l)}) > 1 \end{cases} \quad (9)$$

where γ is a hyper-parameter used here. For simplicity, we **don't tune** γ but set it to 0.1 in all of our experiments by default. Finally, we element-wisely adapt λ according to GSNR of each parameter and get the updating rule for VR-SGD:

$$\theta_t = \theta_{t-1} - \lambda \cdot r(\theta_t) \cdot \tilde{\mathbf{g}}(\theta_t) \quad (10)$$

Figure.1 shows the mechanism of VRGD. As for a good estimation of gradient mean (left panel), optimizer should be confident to move along the direction of gradient mean or even further. However, when gradients on the devices are scatteredly distributed (right panel), updating weights with gradient mean may bring noises and slow down convergence, which should be avoided.

Differences compared with existing LB methods:

- The linear scaling rule uses the same large LR for all parameters, which tends to diverge when some gradients are too large; LARS/LAMB/LANS use large LRs for some layers but layer-wisely or block-wisely limit LRs when $\|\theta_t\|$ is compatible with its updating quantity, i.e., $\|\theta_t\| \sim \|\lambda \cdot \tilde{\mathbf{g}}(\theta_t)\|$; VRGD that we propose here **element-wisely** limits the updating quantity for those parameters without confident gradient estimation (Fig.1b, large gradient variance or small GSNR).
- GSNR and its relationship with generalization gap is discussed in Liu *et al.* [2020a], but further work to embed such GSNR into the optimizers is missing. In our work, we apply GSNR in the SGD/LARS/LAMB and demonstrate that GSNR helps the model maintain a small generalization gap in LB training based on the derivations of the generalization gap and ImageNet experiments.
- VRGD does not need extra-gradient used in EXTRAP-SGD or the two-stage training like SWAP. Sub gradients used in Batch Augmentation have different transforms each while VRGD uses the same transforms. Adasum adaptively sums two gradients scaled by a constant while VRGD still uses the mean gradient.

4.2 VR-Adam, VR-LAMB and other VRGD optimizers

GSNR can be easily applied on any optimizer using the general updating rules shown above. Here we discuss those popular optimizers frequently used in the research community, e.g., SGD, Adam, LARS and LAMB. As for VR-Adam, GSNR is calculated directly based on $\tilde{\mathbf{g}}(\theta_t)$ and then used to adapt the gradient mean before gradients' momentum estimation. Similar with the gradients' momentum, we apply the momentum mechanism on GSNR (\hat{p}_t) for faster convergence. If we adapt the final update term, i.e. $\theta_t \leftarrow \theta_{t-1} - \lambda \cdot r(\theta_t) \cdot \hat{m}_t / (\sqrt{\hat{v}_t} + \varepsilon)$, the 1st and 2nd order momentum estimation (m_t and v_t) for the next training step would be biased (meaning that the update term cannot be inferred merely on \hat{m}_t and \hat{v}_t since $r(\theta_t) \neq 1$).

VR-LAMB is similar to VR-Adam, except that VR-LAMB layer-wisely adapt the LRs for stable convergence when using very large LRs. VR-Adam and VR-LAMB are shown in Appendix.D. VR-LARS and VR-Momentum, which are based on LARS and Momentum, are similar to VR-SGD that it uses GSNR to adapt the gradient means before applying them to the model weights (algorithms omitted).

5 Theoretical Analysis

5.1 Convergence Analysis

Assumption 2 (bounded gradient). $\|\nabla L(\theta)\| \leq G$

Assumption 3 (l -smooth). $\exists l > 0$ satisfies $\|\nabla L(x) - \nabla L(y)\| \leq l\|x - y\|$

We mathematically derive the convergence rate of VR-SGD under nonconvex settings and assume the training process satisfies Assumption.2 and Assumption.3, which are widely used in convergence analysis [Shamir and Zhang, 2013; Ghadimi and Lan, 2013; Allen-Zhu and Hazan, 2016; Allen-Zhu *et al.*, 2019; You *et al.*, 2020]. Table.8 of Appendix compares the assumptions of ours and those popular optimizers. It shows that our assumptions are weaker than LARS/LAMB/DecentLaM and similar with SGD. Then we have Theorem.1. Note that Assumption.2 can be relaxed and all these detailed derivations can be found in Appendix.A.

Theorem 1. Let $\lambda_t = \sqrt{\frac{L(\theta_1) - L(\theta^*)}{T\|\ell\|_1}}$ and $\frac{1}{\sqrt{T}} = \sqrt{\frac{[(L(\theta_1) - L(\theta^*))\|\ell\|_1]}{T}}$, VR-SGD is bounded by:

$$E\|\nabla L(\theta_t)\|^2 \leq \mathcal{O}\left(\left(1 + \frac{r_u^2 G^2}{2}\right) \frac{1}{r_l^2 \sqrt{T}}\right) \quad (11)$$

where r_l and r_u are the lower and upper bound of GSNR.

Convergence rates discussion: 1) The convergence rate $\mathcal{O}(\frac{1}{\sqrt{T}})$ of VR-SGD is the same as SGD [Johnson and Zhang, 2013b]; 2) VR-SGD's bound depends on the lower (r_l) and upper bound (r_u) of GSNR. Larger batch size brings smaller gradient variance (eq.58 of Appendix.B) and larger GSNR (both bigger r_l and r_u), then may result in **a tighter bound with quicker convergence** (verified by experiments shown in Figure.3).

5.2 Generalization Gap

This section derives the generalization gap of SGD and VR-SGD during SB and LB scenarios. Detailed derivations can be found in Appendix.B. Citing eq.14 of Liu *et al.* [2020a] below, i.e., when training satisfies Assumption.1 and $\lambda \rightarrow 0$, after one training step the expectation of empirical generalization gap at t^{th} step is:

$$E_{D, D' \sim \mathcal{Z}^n}(\Delta_t L[D] - \Delta_t L[D']) = \lambda \sum_j \sigma_{t,j}^2 + \mathcal{O}(\lambda^2) \quad (12)$$

where we use $\sigma_{t,j}^2$ and $r_{t,j}$ to denote $\sigma^2(\theta_{t,j})$ and $r(\theta_{t,j})$ for simplicity. Next, we assume that the batch size of LB is k times than that of SB. λ_0 (λ) represents the learning rate of SB (LB). The accumulated generalization gap after training T steps for SB using SGD and T/k steps for LB can be derived as follows:

$$E(\mathbf{GAP}_{SB,SGD}) \approx \lambda_0 \sum_{t=1}^T \sum_j \sigma_{t,j}^2; \quad E(\mathbf{GAP}_{LB,SGD}) \approx \frac{\lambda}{k} \sum_{t=1}^{T/k} \sum_j \sigma_{t,j}^2 \quad (13)$$

If we assume " $\sigma_{t,j}$ is t -independent", eq.13 are simplified as $E(\mathbf{GAP}_{SB,SGD}) \approx \lambda_0 T \sum_j \sigma_j^2$ and $E(\mathbf{GAP}_{LB,SGD}) \approx \frac{\lambda T}{k^2} \sum_j \sigma_j^2$ respectively. Taking $\lambda = k^2 \lambda_0$, $E(\mathbf{GAP}_{LB,SGD})$ will have the same accumulated generalization gap as SB. This is known as the linear/square scaling rules. However, the assumption that " $\sigma_{t,j}$ is t -independent" is unrealistic. Similarly, the accumulated generalization gap of VR-SGD in LB training can be written as:

$$E(\mathbf{GAP}_{LB,VR-SGD}) \approx \sum_{t=1}^{T/k} \sum_j \frac{\lambda r_{t,j} \sigma_{t,j}^2}{k} = \frac{\lambda}{k} \sum_{t=1}^{T/k} \sum_j \mathbf{g}_{t,j}^2 \quad (14)$$

The generalization gap of SGD and VR-SGD in LB training:

When training converges ($\mathbf{g}_{t,j} \rightarrow 0$), we have $\mathbf{g}_{t,j}^2 < \sigma_{t,j}^2$ because $r_{t,j} = \mathbf{g}_{t,j}^2 / \sigma_{t,j}^2 \rightarrow 0$ (verified experimentally by Figure.4 of Liu *et al.* [2020a]). Therefore, we have $\frac{\lambda}{k} \sum_{t=1}^{T/k} \sum_j \mathbf{g}_{t,j}^2 <$

$\frac{\lambda}{k} \sum_{t=1}^{T/k} \sum_j \sigma_{t,j}^2$, i.e., $E(\mathbf{GAP}_{LB,VR-SGD}) < E(\mathbf{GAP}_{LB,SGD})$. This inequality demonstrates that VR-SGD has a **much smaller generalization gap** than SGD in LB training (*verified by BERT and ImageNet experiments*).

Intuitively, Fig.2 shows a schematic to help understanding how GSNR works to reduce generalization gap. It shows that larger GSNR helps the weights to escape from the large generalization gap area, while smaller GSNR attracts the weights to stay in small generalization gap area.

6 Experiments

In this section, we show comprehensive experiments on commonly used LB benchmarks such as BERT Pretraining [Devlin *et al.*, 2019], ImageNet-2012 [Russakovsky *et al.*, 2015] and DLRM [Naumov and Mudigere, 2020]. We mainly adopt the square root rules to scale LR. We set the hyper-parameters of VRGD as $\gamma = 0.1$ and k to the minimum GPU devices that can hold the LB without out of memory for resource efficiency (but satisfy $k \geq 8$) in all experiments. Similar with other optimizers, VRGD can generate a generally good training curve using default sets. The 1st and 2nd order decay rates are set to $\beta_1 = \beta_3 = 0.9$, $\beta_2 = 0.999$ by default. Experiments are performed with TensorFlow on 96 DGX-A100 nodes (768-GPUs).

6.1 BERT Pretraining

BERT pretraining is a common NLP task needs speeding up with LB training. For a fair comparison, we use the same settings as LAMB [You *et al.*, 2020] except optimizer and learning rate: (1) BERT large pretrains using Wikipedia and BooksCorpus and then finetunes on SQuAD(v1.1) to evaluate its precision with F1 score; (2) A two-phase training strategy is used. First 90% steps use a sequence length of 128 (phase-1) and last 10% use a sequence length of 512 (phase-2). Mixed-Batch Training is used when batch size is set to 64k/32k, 96k/32k and 128k/64k.

Table 1: Dev set F1 score of **BERT pretraining and then finetuning on SQuAD(v1.1)**. Each score is the median result of 3 repeated experiments. The baseline of BERT-large on SQuAD(v1.1) is 90.395 [You *et al.*, 2020].

| Batch Size | 16k | 32k | 64k/32k | 64k | 96k/32k | 96k | 128k/32k | 128k/64k |
|---------------------------------------|---------------------------|---------------------------|---------------------------|---------------------------|---------------------------|--------------|----------|--------------|
| Steps | 31250 | 15625 | 8599 | 7820 | 6256 | 5214 | 6137 | 4301 |
| LAMB* [You <i>et al.</i> , 2020] | 91.35 | 91.48 | 90.58 | - | - | - | - | - |
| Adam* [Nado <i>et al.</i> , 2021] | - | 91.58 | 91.04 | 90.46 | - | - | - | - |
| LANS* [Zheng <i>et al.</i> , 2020] | - | - | - | - | 90.60 | - | - | - |
| Adasum* [Maleki <i>et al.</i> , 2021] | - | - | - | - | - | - | 90.50 | - |
| VR-LAMB (ours) | 91.42 (+0.07pp) | 91.58 (+0.00pp) | 91.49 (+0.45pp) | 91.30 (+0.84pp) | 91.23 (+0.63pp) | 90.70 | - | 90.85 |

* means the F1 scores are cited from their work.

Using median of repeated experiments is the same as Nado *et al.* [2021].

We use NVIDIA’s best practise² to carry out VR-LAMB experiments and tune *nothing* of the downstream SQuAD(v1.1) tasks (same as LAMB). Detailed hyper-parameters are listed in Appendix.D. Results shown in Table.1 indicate that:

- VR-LAMB outperforms LAMB (widely used in BERT LB pretraining) in all batch sizes from 16k to 64k/32k. F1 score is improved up to 91.49 at 64k/32k, **0.91pp** higher than LAMB.
- VR-LAMB also outperforms Adam (with standard bias correction and LR discontinuity removal) and LANS by an improvement of **0.84pp** at 64k and **0.63pp** at 96k/32k respectively.
- VR-LAMB pushes the batch size limit up to **128k/64k** using just **4301** steps and maintains a F1 score of 90.85. Although Adasum achieves a F1 score of 90.50 at 128k/32k, but it needs 6137 steps to converge (30% extra steps than VR-LAMB). VR-LAMB achieves 50% less steps than LAMB at 64k/32k and even **0.45pp** higher of F1 score than baseline.

Generalization gap: Table.2 shows that our proposed method can reduce the generalization gap of BERT pretraining by 65.7% when batch size is 64k.

²<https://github.com/NVIDIA/DeepLearningExamples/tree/master>

Table 2: Generalization gap of **BERT pretraining** (64k).

| | LAMB | VR-LAMB(ours) |
|--------------------|------|---------------|
| Train Loss | 1.11 | 1.31 |
| Test Loss | 1.46 | 1.43 |
| Generalization Gap | 0.35 | 0.12(-65.7%) |

As for the wall clock time, training BERT with 128k/64k batch size and 768 GPUs (A100), we can achieve the desired F1 score within 64.1m. More details can be found in the Appendix.E.

6.2 ImageNet with ResNet50

ImageNet training with ResNet50 v1.5 [He *et al.*, 2016a] is a standard CV benchmark for LB training. We use the default sets of official best practise of Google Tensorflow³ with linear LR warm-up, label smoothing and cosine LR decay (to 0). It is the same setup as LARS [Liu *et al.*, 2021]. We merely adjust the optimizers and learning rate for a fair comparison. We find some successful LB applications using Momentum, LAMB and LARS, but not for Adam, AdaGrad or AdamW optimizers [Goyal *et al.*, 2017; You *et al.*, 2020; Liu *et al.*, 2021]. LARS based on Momentum is more fitful on CV tasks. Therefore, we merely apply VR-LARS on ImageNet. Detailed hyper-parameters are listed in the appendix.D.

Table 3: Top-1 test accuracy of **ImageNet** using ResNet50. Each test accuracy of VR-LARS(ours) is averaged over 5 repeated experiments. The standard Top-1 accuracy of MLPerf-v0.5 is 74.9%.

| Batch Size | 2k | 4k | 8k | 16k | 32k | 64k | 96k |
|--|----------------------------|----------------------------|----------------------------|----------------------------|---|----------------------------|----------------------------|
| Momentum* [Goyal <i>et al.</i> , 2017] | 76.51% | 76.44% | 76.26% | - | - | - | - |
| DecentLaM* [Yuan <i>et al.</i> , 2021] | 76.43% | - | 76.19% | 76.73% | 76.22% | - | - |
| LAMB* [You <i>et al.</i> , 2020] | 77.11% | 76.92% | 76.89% | 76.66% | 76.42% | - | - |
| LARS* [Liu <i>et al.</i> , 2021] | - | 76.90% | 76.60% | 76.60% | 76.60% | 75.30% | 74.30% |
| VR-LARS (ours) | 77.14% (+0.03pp) | 77.23% (+0.31pp) | 77.36% (+0.47pp) | 77.27% (+0.54pp) | 76.81% [†] (+0.21pp) | 75.86% (+0.56pp) | 74.82% (+0.52pp) |

* means the results are cited from their work.

[†] LR is not tuned until 64k, which means $LR = 7 \cdot 2^2$ may not be optimal for 32k and can be tuned for further improvement. However, the LARS finetunes the LR from 32k (Fig.6 of Liu *et al.* [2021] or Table.13 of Appendix).

Table 4: Generalization Gap of large batch training on **ImageNet**.

| | LARS* | | | VR-LARS (ours) | | |
|--------------------|-------|-------|-------|-------------------------|-------------------------|-------------------------|
| | 32k | 64k | 96k | 32k | 64k | 96k |
| Train Accuracy | 82.50 | 79.60 | 78.90 | 80.00 | 78.06 | 76.28 |
| Test Accuracy | 76.60 | 75.30 | 74.30 | 76.81 | 75.86 | 74.82 |
| Generalization Gap | 5.90 | 4.30 | 4.60 | 3.12 (-47.1%) | 2.20 (-48.8%) | 1.46 (-68.3%) |

* means the results are cited from [Liu *et al.*, 2021].

Similar phenomenon that train accuracy becomes smaller in VR-LARS is also observed in ConAdv+AA [Liu *et al.*, 2021].

Table 5: Test AUC of **DLRM** trained with SGD and VR-SGD in 1 epoch. The reported results are averaged over 5 repeated experiments. The baseline AUC is 0.8014 for SGD at 32k batch size.

| Batch Size | 32k | 64k | 128k | 256k | 512k |
|------------------|----------------------------|----------------------------|----------------------------|----------------------------|----------------------------|
| SGD [†] | 0.8014 | 0.8025 | 0.8021 | 0.7827 | 0.7787 |
| VR-SGD (ours) | 0.8026 (+0.12pp) | 0.8048 (+0.23pp) | 0.8042 (+0.21pp) | 0.8023 (+1.96pp) | 0.8013 (+2.26pp) |

[†] means we reproduce based on NVIDIA's best practise.

The results shown in Table.3 indicate that:

- VR-LARS outperforms Momentum, DecentLaM, LAMB and LARS (previous SOTA) in all batch sizes (from **0.03pp** to **0.56pp**). The improvements are higher for larger batch size.
- VR-LARS achieves 75.86% accuracy at 64k batch size, **0.56pp** higher than LARS. When batch size reaches up to **96k**, VR-LARS maintains 74.82% accuracy, close to the MLPerf-v0.5 standard (74.9%).

Generalization Gap: Table.4 demonstrates that VR-LARS can dramatically narrow the generalization gap in LB training. The generalization gap is only **1.46** for VR-LARS at 96k (**68.3%** smaller than LARS), even smaller than ConAdv+AA (2.2; Liu *et al.* [2021]). Note that VR-LARS can be used together with ConAdv+AA and other techniques for further improvement.

³<https://github.com/tensorflow/models/tree/r1.13.0>

Similarly, training ImageNet with 96k batch size and 192 GPUs just costs 18.9m. The ideal scenario is to select the optimal batch size that satisfies desired accuracy and computing time.

6.3 DLRM Training

Criteo Terabyte click logs dataset (4 billion records) trained with DLRM is a standard CTR prediction benchmark newly added in MLPerf-v0.7. DLRM is used following NVIDIA’s best practise¹. For a fair comparison, we merely modify LRs and optimizers (hyper-parameters are listed in Appendix.D). Settings of Linear LR warm up, polynomial decay and training with 1 epoch are used by their default set up. Results in Table.5 indicates that:

- VR-SGD outperforms SGD in all batch size settings. Similar with experiments shown above, the improvement of VR-SGD w.r.t SGD increases along with larger batch sizes (from **0.12pp** to **2.26pp**).
- VR-SGD pushes the batch size limit up to 512k and maintains a high AUC of **0.8013**, close to the baseline of 0.8014. Note that Google’s submission of MLPerf v0.7 merely uses a maximum batch size of 64k [Kumar *et al.*, 2021].

7 Ablation Studies

7.1 Orthogonal Experiments

Table 6: Top-1 test accuracy of **CIFAR10** trained with Momentum/Adam/LAMB/LARS optimizers and their corresponding VRGD optimizers using ResNet56. Each test accuracy is averaged over 5 repeated experiments. The reported target accuracy for ResNet56 is 93.03% [He *et al.*, 2016a].

| Batch Size | 256 | 512 | 1k | 2k | 4k | 8k |
|--------------------|----------------------------|----------------------------|----------------------------|-----------------------------|-----------------------------|-----------------------------|
| Momentum† | 93.68% | 93.56% | 93.17% | 92.19% | 17.40% | 14.57% |
| VR-Momentum (ours) | 93.79% (+0.11pp) | 93.71% (+0.15pp) | 93.50% (+0.33pp) | 93.28% (+1.09pp) | 92.70% (+75.30pp) | 90.57% (+76.00pp) |
| Adam† | 91.88% | 92.24% | 92.02% | 91.98% | 59.38% | 20.74% |
| VR-Adam (ours) | 92.46% (+0.58pp) | 92.40% (+0.16pp) | 92.43% (+0.41pp) | 92.10% (+0.12pp) | 91.74% (+32.36pp) | 90.86% (+70.12pp) |
| LAMB† | 92.08% | 92.03% | 91.90% | 92.13% | 58.35% | 15.13% |
| VR-LAMB (ours) | 92.29% (+0.21pp) | 92.34% (+0.31pp) | 92.05% (+0.15pp) | 92.43% (+0.30pp) | 92.04% (+33.69pp) | 91.07% (+75.94pp) |
| LARS† | 92.30% | 92.29% | 92.34% | 82.39% | 27.50% | 12.21% |
| VR-LARS (ours) | 92.35% (+0.05pp) | 92.53% (+0.24pp) | 92.44% (+0.10pp) | 92.79% (+10.40pp) | 92.35% (+64.85pp) | 91.86% (+79.65pp) |

† means we reproduce based on Google TensorFlow’s best practise.

In this section, we demonstrate that GSNR is important in optimization and VRGD can be applicable to most popular optimizers using CIFAR10. During CIFAR10 training with ResNet56 [He *et al.*, 2016a,b], we use the default sets of the official best practice for Google Tensorflow² and mainly add square-root LR scaling rules to perform the 216 composite experiments shown in Figure.3. Additional linear LR warm-up, label smoothing and cosine LR decay (to 0) techniques are used to stabilize LB training experiments shown in Table.6, the same as ImageNet training. Detailed hyper-parameters are listed in Appendix.D. As for the test accuracy curves, Figure.3 shows the averaged composite test accuracy curve of all 216 experiments for the LR-batch size pairs. Training with VR-Momentum/VR-Adam/VR-LAMB converge much faster ($1 \sim 2\times$). As for the final precision, Table.6 demonstrate that VR-Momentum/VR-Adam/VR-LAMB/VR-LARS dramatically outperform Momentum/Adam/LAMB/LARS when batch size is larger than 4k, which demonstrates that VRGD is **applicable** to most popular optimizers in LB training. The improvements of VRGD comparing with their base optimizers grow with the increase of batch size. VRGD optimizers remains convergent when batch size reaches 8k.

7.2 GSNR’s Behaviour

To understand GSNR’s behaviour in VRGD optimizers, we perform the linear regression experiments. The true weights are set to $W_i = i, i \in [1, 10]$ and the corresponding parameters w_i are initialized to

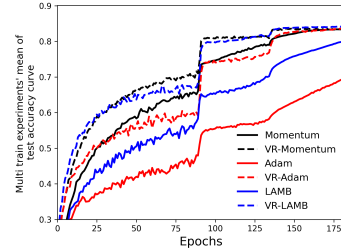


Figure 3: Composite averaged test accuracy or AUC curves of each optimizer for **CIFAR10** experiments. The abrupt surging of accuracy at 91th and 136th epoch is caused by decaying LR with a rate of 0.1.

zero. Given randomly generated inputs X , we have the true labels as $Y = WX$ and the MSE loss as $L = \|Y - wX\|_2$. Finally, optimize w with 100 steps.

Training about 50 (half) steps, VR-SGD is able to converge to the test loss where SGD requires 100 steps (Fig.5a of Appendix.D). The weights of VR-SGD (dashed lines of Fig.5b of Appendix.D) converge faster to their ground truth. We find that w_5, w_6 converge firstly, then w_3, w_8 and finally w_1, w_{10} . Consistently, the GSNR of w_5, w_6 arise firstly (updating w_5, w_6 with larger LR), then w_3, w_8 while the GSNR of w_5, w_6 decrease slowly (no need to update the converged weights using large LR). Finally after step 60, the GSNR of w_1, w_{10} begin to arise. Intuitively, GSNR helps element-wisely fine-tune the LR for different weights.

7.3 Hyper-parameters Sensitivity

There are two main hyper-parameters in VRGD, i.e., normalization strength factor γ and the equivalent GPU device number k . We take use of linear regression trained with VR-SGD using $batchsize = 2048$ shown above to examine the hyper-parameter sensitivity.

Figure.4 shows that the optimal γ is around (0.04, 0.2) for linear regression. Test loss would be larger if $\gamma \rightarrow 1$, which means **VR-SGD is reduced to SGD**. It again demonstrates that GSNR is valuable to improve final precision. On the other hand, the optimal k is around [32, 256]. This means that each gradient mean calculated using [8, 64] samples on each GPU/TPU device, and gradient variance calculated using [32, 256] values of the gradient mean will return a good evaluation of GSNR. In fact, we do not use the optimal hyper-parameters. Instead, above experiments use $\gamma = 0.1$ and set k to the minimum GPU devices that can hold the LB without out of memory (but satisfy $k \geq 8$, refer all of the hyper-parameters in Appendix.D). Fine-tuning γ and k may further improve the results.

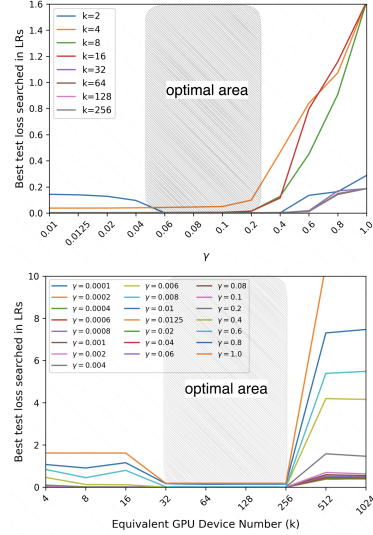


Figure 4: **Hyper parameter sensitivity** experiments: test loss of various γ (Upper panel) and k (Bottom panel).

8 Summary and Discussion

8.1 Summary

In this paper, we propose the VRGD for large batch training using GSNR. We carry out theoretical derivations of convergence rate and generalization analysis to explain why VRGD can accelerate large batch training and reduce generalization gap. Comprehensive experiments on BERT-pretraining, ImageNet and DLRM verify that VRGD can push the batch size limit than previous SOTA optimizers in LB training and perform better. Codes will be released when published.

8.2 Why VRGD scales batch size?

We discuss the reasons why our proposed method can scale the batch size under methodological, convergence rate, Generalization gap and GSNR effectiveness perspectives.

1. Methodological perspective. Our proposed method provides an element-wise level of learning rate adjustment that is more accurate than existing methods and becomes more accurate when batch size gets larger. The linear scaling rule uses the same large LR for all parameters. LARS/LAMB/LANS use large LR for the normal layers but layer-wisely or block-wisely limit LR when $\|\theta_t\|$ is compatible with its updating quantity. VRGD that we proposed **element-wisely** limits the updating quantity for those parameters without confident gradient estimation (Fig.1b in the main context, large gradient variance or small GSNR). GSNR estimation becomes more accurate when batch size is larger. Therefore, when batch size gets extremely large, such mechanism to stabilize training may become even more accurate and helpful.

2. Convergence rate perspective. Applying our proposed method on basic optimizers may make the upper bound of convergence rate much tighter when increasing the batch size. For example, VR-SGD's bound depends on the lower (r_l) and upper bound (r_u) of GSNR. Larger batch size brings

smaller gradient variance (eq.58 of Appendix.B) and larger GSNR (both bigger r_l and r_u), then may result in a **tighter bound with quicker convergence** (*verified by experiments*).

3. Generalization gap perspective. Our proposed method can reduce more generalization gap when batch size is larger. Based on the derivations in Sec 5.2, VR-SGD has a **much smaller generalization gap** than SGD in LB training (*verified by our ImageNet experiments shown in Table.3 of the main context*). When scaling up the batch size, such mechanism to reduce generalization becomes even more useful. Table.3 of the the main context shows that generalization gap drops 47.1% at 32k, 48.8% at 64k and 68.3% at 96k.

4. GSNR effectiveness perspective. The theoretical explanation of the mechanism how updating weights with smaller GSNR brings generalization gap is comprehensively discussed in previous study [Liu *et al.*, 2020a]. We further carried out many ablation studies in Sec.7 and found that final accuracy drops in large batch training without GSNR, which demonstrates its effectiveness in large batch scenarios.

8.3 Comparison with SAM family

Our proposed method is mainly based on generalization gap, but not a straightforward method to escape sharp minimum like SAM [Foret *et al.*, 2021]. We compare our proposed method with SAM family in Table.7. Results show that our proposed method performs better than SAM/ASAM/ESAM/Gradient norm and the same as GSAM [Kwon *et al.*, 2021; Zhuang *et al.*, 2022; Zhao *et al.*, 2022; Du *et al.*, 2022; Liu *et al.*, 2022].

Table 7: Top-1 training accuracy of ImageNet-1k with ResNet50.

| Batch Size | 512 | 4k |
|-----------------------------------|--|--|
| baseline w.o. SAM | 75.8% [Kwon <i>et al.</i> , 2021] | 76.0% [Zhuang <i>et al.</i> , 2022] |
| SAM (90 epochs) | - | 76.9% [Zhuang <i>et al.</i> , 2022] |
| SAM (100 epochs) | 76.4% [Kwon <i>et al.</i> , 2021] | - |
| ASAM (100 epochs) | 76.6% [Kwon <i>et al.</i> , 2021] | - |
| GSAM (90 epochs) | - | 77.2% [Zhuang <i>et al.</i> , 2022] |
| ESAM (90 epochs) | 77.1% [Du <i>et al.</i> , 2022] | - |
| Gradient Norm (100 epochs) | - | 77.1% [Zhao <i>et al.</i> , 2022] |
| Ours (90 epochs) | - | 77.2% |

References

- Zeyuan Allen-Zhu and Elad Hazan. Variance reduction for faster non-convex optimization. In *International conference on machine learning*, pages 699–707. PMLR, 2016.
- Zeyuan Allen-Zhu, Yuanzhi Li, and Zhao Song. A convergence theory for deep learning via over-parameterization. In *International Conference on Machine Learning*, pages 242–252. PMLR, 2019.
- Francis R. Bach and Eric Moulines. Non-asymptotic analysis of stochastic approximation algorithms for machine learning. In John Shawe-Taylor, Richard S. Zemel, Peter L. Bartlett, Fernando C. N. Pereira, and Kilian Q. Weinberger, editors, *Advances in Neural Information Processing Systems 24: 25th Annual Conference on Neural Information Processing Systems 2011. Proceedings of a meeting held 12-14 December 2011, Granada, Spain*, pages 451–459, 2011.
- Jeremy Bernstein, Yu-Xiang Wang, Kamyar Azizzadenesheli, and Animashree Anandkumar. signsgd: Compressed optimisation for non-convex problems. In *International Conference on Machine Learning*, pages 560–569. PMLR, 2018.
- Rishi Bommasani, Drew A Hudson, Ehsan Adeli, Russ Altman, Simran Arora, Sydney von Arx, Michael S Bernstein, Jeannette Bohg, Antoine Bosselut, Emma Brunskill, et al. On the opportunities and risks of foundation models. *arXiv preprint arXiv:2108.07258*, 2021.
- Xiaowu Dai and Yuhua Zhu. Towards theoretical understanding of large batch training in stochastic gradient descent. *CoRR*, abs/1812.00542, 2018.

- Aditya Devarakonda, Maxim Naumov, and Michael Garland. Adabatch: Adaptive batch sizes for training deep neural networks. *arXiv preprint arXiv:1712.02029*, 2017.
- Jacob Devlin, Ming-Wei Chang, Kenton Lee, and Kristina Toutanova. BERT: pre-training of deep bidirectional transformers for language understanding. In Jill Burstein, Christy Doran, and Thamar Solorio, editors, *Proceedings of the 2019 Conference of the North American Chapter of the Association for Computational Linguistics: Human Language Technologies, NAACL-HLT*, pages 4171–4186. Association for Computational Linguistics, 2019.
- Jiawei Du, Hanshu Yan, Jiashi Feng, Joey Tianyi Zhou, Liangli Zhen, Rick Siow Mong Goh, and Vincent Y. F. Tan. Efficient sharpness-aware minimization for improved training of neural networks. In *The Tenth International Conference on Learning Representations, ICLR 2022, Virtual Event, April 25-29, 2022*. OpenReview.net, 2022.
- William Fedus, Barret Zoph, and Noam Shazeer. Switch transformers: Scaling to trillion parameter models with simple and efficient sparsity. *arXiv preprint arXiv:2101.03961*, 2021.
- Luciano Floridi and Massimo Chiriatti. Gpt-3: Its nature, scope, limits, and consequences. *Minds and Machines*, 30(4):681–694, 2020.
- Pierre Foret, Ariel Kleiner, Hossein Mobahi, and Behnam Neyshabur. Sharpness-aware minimization for efficiently improving generalization. In *9th International Conference on Learning Representations, ICLR 2021, Virtual Event, Austria, May 3-7, 2021*. OpenReview.net, 2021.
- Saeed Ghadimi and Guanghui Lan. Stochastic first- and zeroth-order methods for nonconvex stochastic programming. *SIAM J. Optim.*, 23(4):2341–2368, 2013.
- Priya Goyal, Piotr Dollár, Ross Girshick, Pieter Noordhuis, Lukasz Wesolowski, Aapo Kyrola, Andrew Tulloch, Yangqing Jia, and Kaiming He. Accurate, large minibatch sgd: Training imagenet in 1 hour. *arXiv preprint arXiv:1706.02677*, 2017.
- Vipul Gupta, Santiago Aklé Serrano, and Dennis DeCoste. Stochastic weight averaging in parallel: Large-batch training that generalizes well. In *8th International Conference on Learning Representations, ICLR*. OpenReview.net, 2020.
- Kaiming He, Xiangyu Zhang, Shaoqing Ren, and Jian Sun. Deep residual learning for image recognition. In *Proceedings of the IEEE conference on computer vision and pattern recognition*, pages 770–778, 2016.
- Kaiming He, Xiangyu Zhang, Shaoqing Ren, and Jian Sun. Identity mappings in deep residual networks. In *European conference on computer vision*, pages 630–645. Springer, 2016.
- Elad Hoffer, Itay Hubara, and Daniel Soudry. Train longer, generalize better: closing the generalization gap in large batch training of neural networks. In Isabelle Guyon, Ulrike von Luxburg, Samy Bengio, Hanna M. Wallach, Rob Fergus, S. V. N. Vishwanathan, and Roman Garnett, editors, *Advances in Neural Information Processing Systems*, pages 1731–1741, 2017.
- Elad Hoffer, Tal Ben-Nun, Itay Hubara, Niv Giladi, Torsten Hoefer, and Daniel Soudry. Augment your batch: better training with larger batches. *arXiv preprint arXiv:1901.09335*, 2019.
- Zhouyuan Huo, Bin Gu, and Heng Huang. Large batch optimization for deep learning using new complete layer-wise adaptive rate scaling. In *Thirty-Fifth AAAI Conference on Artificial Intelligence, AAAI*, pages 7883–7890. AAAI Press, 2021.
- Rie Johnson and Tong Zhang. Accelerating stochastic gradient descent using predictive variance reduction. *Advances in neural information processing systems*, 26, 2013.
- Rie Johnson and Tong Zhang. Accelerating stochastic gradient descent using predictive variance reduction. In Christopher J. C. Burges, Léon Bottou, Zoubin Ghahramani, and Kilian Q. Weinberger, editors, *Advances in Neural Information Processing Systems 26: 27th Annual Conference on Neural Information Processing Systems 2013. Proceedings of a meeting held December 5-8, 2013, Lake Tahoe, Nevada, United States*, pages 315–323, 2013.

- Nitish Shirish Keskar, Dheevatsa Mudigere, Jorge Nocedal, Mikhail Smelyanskiy, and Ping Tak Peter Tang. On large-batch training for deep learning: Generalization gap and sharp minima. In *5th International Conference on Learning Representations, ICLR*. OpenReview.net, 2017.
- Diederik P. Kingma and Jimmy Ba. Adam: A method for stochastic optimization. In Yoshua Bengio and Yann LeCun, editors, *3rd International Conference on Learning Representations, ICLR*, 2015.
- Sameer Kumar, Yu Emma Wang, Cliff Young, James Bradbury, Naveen Kumar, Dehao Chen, and Andy Swing. Exploring the limits of concurrency in ML training on google TPUS. In Alex Smola, Alex Dimakis, and Ion Stoica, editors, *Proceedings of Machine Learning and Systems 2021, MLSys 2021, virtual, April 5-9, 2021*. mlsys.org, 2021.
- Jungmin Kwon, Jeongseop Kim, Hyunseo Park, and In Kwon Choi. ASAM: adaptive sharpness-aware minimization for scale-invariant learning of deep neural networks. In Marina Meila and Tong Zhang, editors, *Proceedings of the 38th International Conference on Machine Learning, ICML 2021, 18-24 July 2021, Virtual Event*, volume 139 of *Proceedings of Machine Learning Research*, pages 5905–5914. PMLR, 2021.
- Tao Lin, Lingjing Kong, Sebastian Stich, and Martin Jaggi. Extrapolation for large-batch training in deep learning. In *International Conference on Machine Learning*, pages 6094–6104. PMLR, 2020.
- Junyang Lin, Rui Men, An Yang, Chang Zhou, Ming Ding, Yichang Zhang, Peng Wang, Ang Wang, Le Jiang, Xianyan Jia, et al. M6: A chinese multimodal pretrainer. *arXiv preprint arXiv:2103.00823*, 2021.
- Jinlong Liu, Guoqing Jiang, Yunzhi Bai, Ting Chen, and Huayan Wang. Understanding why neural networks generalize well through GSNR of parameters. In *8th International Conference on Learning Representations, ICLR*. OpenReview.net, 2020.
- Yanli Liu, Kaiqing Zhang, Tamer Basar, and Wotao Yin. An improved analysis of (variance-reduced) policy gradient and natural policy gradient methods. *Advances in Neural Information Processing Systems*, 33:7624–7636, 2020.
- Yong Liu, Xiangning Chen, Minhao Cheng, Cho-Jui Hsieh, and Yang You. Concurrent adversarial learning for large-batch training. *arXiv preprint arXiv:2106.00221*, 2021.
- Yong Liu, Siqi Mai, Xiangning Chen, Cho-Jui Hsieh, and Yang You. Towards efficient and scalable sharpness-aware minimization. In *IEEE/CVF Conference on Computer Vision and Pattern Recognition, CVPR 2022, New Orleans, LA, USA, June 18-24, 2022*, pages 12350–12360. IEEE, 2022.
- Saeed Maleki, Madan Musuvathi, Todd Mytkowicz, Olli Saarikivi, Tianju Xu, Vadim Eksarevskiy, Jaliya Ekanayake, and Emad Barsoum. Scaling distributed training with adaptive summation. In Alex Smola, Alex Dimakis, and Ion Stoica, editors, *Proceedings of Machine Learning and Systems 2021, MLSys 2021, virtual, April 5-9, 2021*. mlsys.org, 2021.
- Sam McCandlish, Jared Kaplan, Dario Amodei, and OpenAI Dota Team. An empirical model of large-batch training. *CoRR*, abs/1812.06162, 2018.
- Andrew Miller, Nick Foti, Alexander D’Amour, and Ryan P Adams. Reducing reparameterization gradient variance. *Advances in Neural Information Processing Systems*, 30, 2017.
- Zachary Nado, Justin M Gilmer, Christopher J Shallue, Rohan Anil, and George E Dahl. A large batch optimizer reality check: Traditional, generic optimizers suffice across batch sizes. *arXiv preprint arXiv:2102.06356*, 2021.
- Maxim Naumov and Dheevatsa Mudigere. Dlrn: An advanced, open source deep learning recommendation model, 2020.
- Lam M. Nguyen, Phuong Ha Nguyen, Marten van Dijk, Peter Richtárik, Katya Scheinberg, and Martin Takáč. SGD and hogwild! convergence without the bounded gradients assumption. In Jennifer G. Dy and Andreas Krause, editors, *Proceedings of the 35th International Conference on Machine Learning, ICML 2018, Stockholmsmässan, Stockholm, Sweden, July 10-15, 2018*, volume 80 of *Proceedings of Machine Learning Research*, pages 3747–3755. PMLR, 2018.

- Matteo Papini, Damiano Binaghi, Giuseppe Canonaco, Matteo Pirotta, and Marcello Restelli. Stochastic variance-reduced policy gradient. In *International conference on machine learning*, pages 4026–4035. PMLR, 2018.
- Tom Rainforth, Adam R. Kosiorek, Tuan Anh Le, Chris J. Maddison, Maximilian Igl, Frank Wood, and Yee Whye Teh. Tighter variational bounds are not necessarily better. In Jennifer G. Dy and Andreas Krause, editors, *Proceedings of the 35th International Conference on Machine Learning, ICML*, volume 80 of *Proceedings of Machine Learning Research*, pages 4274–4282. PMLR, 2018.
- Olga Russakovsky, Jia Deng, Hao Su, Jonathan Krause, Sanjeev Satheesh, Sean Ma, Zhiheng Huang, Andrej Karpathy, Aditya Khosla, Michael Bernstein, Alexander C. Berg, and Li Fei-Fei. ImageNet Large Scale Visual Recognition Challenge. *International Journal of Computer Vision (IJCV)*, 115(3):211–252, 2015.
- Christopher De Sa. Cs4787: Principles of large-scale machine learning. 2021.
- Ohad Shamir and Tong Zhang. Stochastic gradient descent for non-smooth optimization: Convergence results and optimal averaging schemes. In *International conference on machine learning*, pages 71–79. PMLR, 2013.
- Samuel L. Smith, Pieter-Jan Kindermans, Chris Ying, and Quoc V. Le. Don’t decay the learning rate, increase the batch size. In *6th International Conference on Learning Representations, ICLR*. OpenReview.net, 2018.
- Chong Wang, Xi Chen, Alexander J Smola, and Eric P Xing. Variance reduction for stochastic gradient optimization. *Advances in Neural Information Processing Systems*, 26, 2013.
- Yang You, Igor Gitman, and Boris Ginsburg. Large batch training of convolutional networks. *arXiv preprint arXiv:1708.03888*, 2017.
- Yang You, Igor Gitman, and Boris Ginsburg. Scaling sgd batch size to 32k for imagenet training. *arXiv preprint arXiv:1708.03888*, 6(12):6, 2017.
- Yang You, Jing Li, Sashank J. Reddi, Jonathan Hseu, Sanjiv Kumar, Srinadh Bhojanapalli, Xiaodan Song, James Demmel, Kurt Keutzer, and Cho-Jui Hsieh. Large batch optimization for deep learning: Training BERT in 76 minutes. In *8th International Conference on Learning Representations, ICLR*. OpenReview.net, 2020.
- Kun Yuan, Yiming Chen, Xinmeng Huang, Yingya Zhang, Pan Pan, Yinghui Xu, and Wotao Yin. Decentlam: Decentralized momentum SGD for large-batch deep training. In *2021 IEEE/CVF International Conference on Computer Vision, ICCV 2021, Montreal, QC, Canada, October 10-17, 2021*, pages 3009–3019. IEEE, 2021.
- Yang Zhao, Hao Zhang, and Xiuyuan Hu. Penalizing gradient norm for efficiently improving generalization in deep learning. In Kamalika Chaudhuri, Stefanie Jegelka, Le Song, Csaba Szepesvári, Gang Niu, and Sivan Sabato, editors, *International Conference on Machine Learning, ICML 2022, 17-23 July 2022, Baltimore, Maryland, USA*, volume 162 of *Proceedings of Machine Learning Research*, pages 26982–26992. PMLR, 2022.
- Shuai Zheng, Haibin Lin, Sheng Zha, and Mu Li. Accelerated large batch optimization of BERT pretraining in 54 minutes. *CoRR*, abs/2006.13484, 2020.
- Juntang Zhuang, Boqing Gong, Liangzhe Yuan, Yin Cui, Hartwig Adam, Nicha C. Dvornek, Sekhar Tatikonda, James S. Duncan, and Ting Liu. Surrogate gap minimization improves sharpness-aware training. In *The Tenth International Conference on Learning Representations, ICLR 2022, Virtual Event, April 25-29, 2022*. OpenReview.net, 2022.

A Proof of VR-SGD’s convergence rate:

Our assumptions are weaker than LARS/LAMB/DecentLaM and similar with SGD. We assume that the training process satisfies Assumption.2 and Assumption.3, which are widely used in famous optimizers (Table.8). Our derivations does not require the bounded variance. We confine the bound of GSNR to $r(\theta) \leq 1$. GSNR upper bound is not strong and may exist in practise, e.g., Liu *et al.* [2020a] found that GSNR will first grow and than decay over time. Layer level bound is also used in the derivations of LARS/LAMB[You *et al.*, 2020] and such assumption can be inferred under the overall bound. For example, if it satisfies $\|\nabla L(\theta)\| \leq G_{max}$, then $\exists G_i \leq G_{max}, i \in (1, 2, \dots, h)$ satisfy $\|\nabla L_i(\theta)\| \leq G_i$. We define the expectation of stochastic mini-batch gradient as the true gradient, i.e., $E(\mathbf{g}^{(i)}) = \nabla_i L(\theta)$. Note that bounded gradient assumption can be **relaxed** (last part of Appendix.A).

Table 8: Assumptions comparing with widely used optimizers.

| Optimizer | Assumption.1 (bounded gradient) | Assumption.2 (l -smooth) | Other assumption (bounded variance) |
|--------------------------------------|------------------------------------|--------------------------------|--|
| SGD[Sa, 2021] | ✓ | ✓ | × |
| Adam[Kingma and Ba, 2015] | ✓ | × | × |
| SVRG[Johnson and Zhang, 2013b] | × | ✓ | × |
| LARS[You <i>et al.</i> , 2020] | ✓ | ✓ | ✓ |
| LAMB[You <i>et al.</i> , 2020] | ✓ | ✓ | ✓ |
| EXTRAP-SGD[Lin <i>et al.</i> , 2020] | × | ✓ | ✓ |
| DecentLaM[Yuan <i>et al.</i> , 2021] | ✓ | ✓ | ✓ |
| VR-SGD(ours) | ✓ | ✓ | × |

Proof. Inspired by [Sa, 2021; You *et al.*, 2020; Shamir and Zhang, 2013; Ghadimi and Lan, 2013; Allen-Zhu and Hazan, 2016; Allen-Zhu *et al.*, 2019], the convergence of VR-SGD under general nonconvex setting is derived below. VR-SGD’s updating rule is:

$$\theta_{t+1}^{(i)} = \theta_t^{(i)} - \lambda_t \cdot r_t^{(i)} \cdot \mathbf{g}_t^{(i)} \quad (15)$$

where $\theta_t^{(i)}$ represents the i^{th} layer parameters of the model at t^{th} training step, $r_t^{(i)}$ and $\mathbf{g}_t^{(i)}$ represents the corresponding GSNR and gradient mean.

From Taylor’s theorem and Assumption.3, there exists the upper quadratic bound:

$$L(\theta_{t+1}) \leq L(\theta_t) + \underbrace{< \nabla_i L(\theta_t), \theta_{t+1}^{(i)} - \theta_t^{(i)} >}_{T_1} + \underbrace{\sum_{i=1}^h \frac{\ell_i}{2} \|\theta_{t+1}^{(i)} - \theta_t^{(i)}\|^2}_{T_2} \quad (16)$$

The 2^{nd} term T_2 of eq.(16):

$$T_2 = \sum_{i=1}^h \frac{\ell_i}{2} \|\theta_{t+1}^{(i)} - \theta_t^{(i)}\|^2 \quad (17)$$

$$= \sum_{i=1}^h \frac{\ell_i}{2} (-\lambda_t \cdot r_t^{(i)} \cdot \mathbf{g}_t^{(i)})^2 \quad (18)$$

Applying the GSNR definition $r_t^{(i)} := \frac{\mathbf{g}_t^{2(i)}}{\sigma_t^{2(i)}}$, we have:

$$T_2 = \frac{\lambda_t^2}{2} \sum_{i=1}^h \ell_i \frac{[\mathbf{g}_t^{(i)}]^6}{[\sigma_t^{(i)}]^4} \quad (19)$$

Taking expectation, we have:

$$E(T_2) \leq \frac{\lambda_t^2 r_u^2 G^2 \|\ell\|_1}{2} \quad (20)$$

The 1st term T_1 of eq.(16):

$$T_1 = \langle \nabla_i L(\theta_t), \theta_{t+1}^{(i)} - \theta_t^{(i)} \rangle \quad (21)$$

$$= -\lambda_t \sum_{i=1}^h \sum_{j=1}^{d_i} [\nabla_i L(\theta_t)]_j \cdot \frac{[\mathbf{g}_{t,j}^{(i)}]^3}{[\sigma_{t,j}^{(i)}]^2} \quad (22)$$

$$\leq \underbrace{-\lambda_t r_l^2 \sum_{i=1}^h \sum_{j=1}^{d_i} \left([\nabla_i L(\theta_t)]_j \cdot [\mathbf{g}_{t,j}^{(i)}] \right)}_{T_3} \quad (23)$$

$$+ \underbrace{\lambda_t \sum_{i=1}^h \sum_{j=1}^{d_i} \left([\nabla_i L(\theta_t)]_j \cdot \frac{[\mathbf{g}_{t,j}^{(i)}]^3}{[\sigma_{t,j}^{(i)}]^2} \mathbf{1}(\text{sign}[\nabla_i] \neq \text{sign}[\mathbf{g}^{(i)}]) \right)}_{T_4} \quad (24)$$

where $\mathbf{1}(\text{sign}[\nabla_i] \neq \text{sign}[\mathbf{g}^{(i)}]) = \mathbf{1}(\text{sign}([\nabla_i L(\theta_t)]_j) \neq \text{sign}(\mathbf{g}_{t,j}^{(i)}))$.

Taking expectation of T_3 and T_4 , we have:

$$E(T_3) = -\lambda_t r_l^2 \sum_{i=1}^h \sum_{j=1}^{d_i} E \left([\nabla_i L(\theta_t)]_j \cdot [\mathbf{g}_{t,j}^{(i)}] \right) \quad (25)$$

$$= -\lambda_t r_l^2 \|\nabla L(\theta_t)\|^2 \quad (26)$$

$$E(T_4) = \lambda_t \sum_{i=1}^h \sum_{j=1}^{d_i} E \left([\nabla_i L(\theta_t)]_j \cdot \frac{[\mathbf{g}_{t,j}^{(i)}]^3}{[\sigma_{t,j}^{(i)}]^2} \cdot \mathbf{1}(\text{sign}([\nabla_i L(\theta_t)]_j) \neq \text{sign}(\mathbf{g}_{t,j}^{(i)})) \right) \quad (27)$$

$$= \lambda_t \sum_{i=1}^h \sum_{j=1}^{d_i} E \left([\nabla_i L(\theta_t)]_j \cdot \frac{[\mathbf{g}_{t,j}^{(i)}]^3}{[\sigma_{t,j}^{(i)}]^2} \mid \mathbf{P}(\text{sign}([\nabla_i L(\theta_t)]_j) \neq \text{sign}(\mathbf{g}_{t,j}^{(i)})) \right) \quad (28)$$

The probability is bounded by relaxing the condition, then using Markov's and finally Jensen's inequality (inspired by Sign-SGD[Bernstein *et al.*, 2018; Nado *et al.*, 2021]):

$$\mathbf{P}(\text{sign}([\nabla_i L(\theta_t)]_j) \neq \text{sign}(\mathbf{g}_{t,j}^{(i)})) \quad (29)$$

$$\leq \mathbf{P} \left(|[\nabla_i L(\theta_t)]_j - \mathbf{g}_{t,j}^{(i)}| \geq |[\nabla_i L(\theta_t)]_j| \right) \quad (30)$$

$$\leq \frac{E \left[|[\nabla_i L(\theta_t)]_j - \mathbf{g}_{t,j}^{(i)}| \right]}{|[\nabla_i L(\theta_t)]_j|} \quad (31)$$

$$\leq \frac{\sqrt{E \left[([\nabla_i L(\theta_t)]_j - \mathbf{g}_{t,j}^{(i)})^2 \right]}}{|[\nabla_i L(\theta_t)]_j|} \quad (32)$$

$$= \frac{\sigma_{t,j}^{(i)}}{|[\nabla_i L(\theta_t)]_j|} \quad (33)$$

Substituting this relation into T_4 , we have

$$E(T_4) \leq \lambda_t \sum_{i=1}^h \sum_{j=1}^{d_i} E \left[[\nabla_i L(\theta_t)]_j \cdot \frac{[\mathbf{g}_{t,j}^{(i)}]^3}{[\sigma_{t,j}^{(i)}]^2} \cdot \frac{\sigma_{t,j}^{(i)}}{|[\nabla_i L(\theta_t)]_j|} \right] \quad (34)$$

$$\leq \lambda_t \sum_{i=1}^h \sum_{j=1}^{d_i} E \left[\frac{[\mathbf{g}_{t,j}^{(i)}]^3}{\sigma_{t,j}^{(i)}} \right] \quad (35)$$

$$\leq \lambda_t r_u^{\frac{1}{2}} G^2 \quad (36)$$

Rearranging eq.(16) and taking expectation, we have:

$$E[L(\theta_{t+1})] \leq E[L(\theta_t)] - \lambda_t r_l^2 \|\nabla L(\theta_t)\|^2 + \lambda_t r_u^{\frac{1}{2}} G^2 + \frac{\lambda_t^2 r_u^2 G^2 \|\ell\|_1}{2} \quad (37)$$

$$= E[L(\theta_t)] - \lambda_t r_l^2 \|\nabla L(\theta_t)\|^2 + \lambda_t r_u^{\frac{1}{2}} G^2 \cdot \left(1 + \frac{\lambda_t r_u^{\frac{3}{2}} \|\ell\|_1}{2}\right) \quad (38)$$

Summing this until step T , we have:

$$E[L(\theta_{T+1})] \leq L(\theta_1) - \lambda_t r_l^2 \sum_{t=1}^T \|\nabla L(\theta_t)\|^2 + T \lambda_t r_u^{\frac{1}{2}} G^2 \cdot \left(1 + \frac{\lambda_t r_u^{\frac{3}{2}} \|\ell\|_1}{2}\right) \quad (39)$$

Rearranging this and assuming θ^* to be the optimal model parameters satisfies $L(\theta^*) \leq E[L(\theta_{T+1})]$:

$$\frac{1}{T} \sum_{t=1}^T \|\nabla L(\theta_t)\|^2 \leq \frac{1}{r_l^2} \left[\frac{L(\theta_1) - E[L(\theta_{T+1})]}{\lambda_t T} + r_u^{\frac{1}{2}} G^2 \cdot \left(1 + \frac{\lambda_t r_u^{\frac{3}{2}} \|\ell\|_1}{2}\right) \right] \quad (40)$$

$$\leq \frac{1}{r_l^2} \left[\frac{L(\theta_1) - L(\theta^*)}{\lambda_t T} + r_u^{\frac{1}{2}} G^2 \cdot \left(1 + \frac{\lambda_t r_u^{\frac{3}{2}} \|\ell\|_1}{2}\right) \right] \quad (41)$$

Taking $\lambda_t = \sqrt{\frac{L(\theta_1) - L(\theta^*)}{T \|\ell\|_1}}$, we can get the bound of VR-SGD:

$$E\|\nabla L(\theta_t)\|^2 \leq \frac{1}{r_l^2} \left[\sqrt{\frac{[L(\theta_1) - L(\theta^*)] \|\ell\|_1}{T}} + r_u^{\frac{1}{2}} G^2 \left(1 + \frac{r_u^{\frac{3}{2}}}{2} \sqrt{\frac{[L(\theta_1) - L(\theta^*)] \|\ell\|_1}{T}}\right) \right] \quad (42)$$

Denoting $\frac{1}{\sqrt{\hat{T}}} = \sqrt{\frac{[L(\theta_1) - L(\theta^*)] \|\ell\|_1}{T}}$, we have:

$$E\|\nabla L(\theta_t)\|^2 \leq \mathcal{O} \left(\left(1 + \frac{r_u^2 G^2}{2}\right) \frac{1}{r_l^2 \sqrt{\hat{T}}} \right) \quad (43)$$

Furthermore, **the bounded gradients assumption can be relaxed**. Bach and Moulines [2011] (their Theorem.4) and Nguyen *et al.* [2018] (their Lemma.2) derived that SGD can still be bounded without bounded gradients assumption, but they still needed the l -smooth assumption.

Based on the derivations of Theorem.1 in Johnson and Zhang [2013a], we can derive a similar bound for our proposed method without bounded gradients assumption by taking $\lambda = \frac{1}{\sqrt{T}}$, we have

$$E\|\nabla L(\theta_t)\|^2 \leq \left[\frac{1}{\gamma r_l (\sqrt{T} - 2l)} + \frac{2l}{\sqrt{T} - 2l} \right] E[L(\theta_t) - L(\theta_*)] \quad (44)$$

Therefore, when λ gradually decreases with T , our proposed method still converges with $O(\frac{1}{\sqrt{T}})$ without bounded gradient assumption.

B Generalization Gap Derivations of SGD and VR-SGD in LB Scenarios

Inspired by [Liu *et al.*, 2020a], the generalization gap of SB and LB using SGD and VR-SGD is derived below. Firstly, the derivations of one step generalization gap are briefly reviewed below and the detailed derivations can be reached in [Liu *et al.*, 2020a]. The gradient mean over training set D is denoted as $\mathbf{g}_D(\theta)$. $\mathbf{g}_i(\theta)$ denotes the gradient of a single data sample and $\tilde{\mathbf{g}}(\theta)$ to denote its expectation over the entire data distribution. Similarly we denote $\mathbf{g}_{D'}(\theta)$ as the gradient mean over test set D' .

$$\begin{aligned} \mathbf{g}_D(\theta) &= \frac{1}{n} \sum_{i=1}^n \mathbf{g}(x_i, y_i, \theta) = \frac{\partial L[D]}{\partial \theta} \\ \mathbf{g}_{D'}(\theta) &= \frac{1}{n'} \sum_{i=1}^{n'} \mathbf{g}(x'_i, y'_i, \theta) = \frac{\partial L[D']}{\partial \theta} \end{aligned} \quad (45)$$

Using Assumption 0.0.1 in the main context, we have:

$$E_{D \sim \mathcal{Z}^n}[\mathbf{g}_D(\theta)] = E_{D, D' \sim \mathcal{Z}^n}[\mathbf{g}_{D'}(\theta)] = \tilde{\mathbf{g}}(\theta) \quad (46)$$

$$\text{Var}_{D \sim \mathcal{Z}^n}[\mathbf{g}_D(\theta)] = \sigma^2(\theta) \quad (47)$$

After one training step, the model parameters are updated by $\Delta\theta = -\lambda \mathbf{g}_D(\theta)$. If λ is small enough, the reduction in one-step training and test loss can be approximated as:

$$\begin{aligned} \Delta L[D] &\approx -\Delta\theta \cdot \frac{\partial L[D]}{\partial \theta} + O(\lambda^2) \\ &= \lambda \mathbf{g}_D(\theta) \cdot \mathbf{g}_D(\theta) + O(\lambda^2) \end{aligned} \quad (48)$$

$$\begin{aligned} \Delta L[D'] &\approx -\Delta\theta \cdot \frac{\partial L[D']}{\partial \theta} + O(\lambda^2) \\ &= \lambda \mathbf{g}_D(\theta) \cdot \mathbf{g}_{D'}(\theta) + O(\lambda^2) \end{aligned} \quad (49)$$

Empirically, $\Delta L[D]$ will be larger than $\Delta L[D']$, and the generalization gap will gradually increase. When $\lambda \rightarrow 0$, after one single training step the empirical generalization gap is denoted as ∇ for simplicity. Therefore we have

$$\nabla := \Delta L[D] - \Delta L[D'] \quad (50)$$

$$\approx \lambda \mathbf{g}_D(\theta) \cdot \mathbf{g}_D(\theta) - \lambda \mathbf{g}_D(\theta) \cdot \mathbf{g}_{D'}(\theta) \quad (51)$$

$$= \lambda(\tilde{\mathbf{g}}(\theta) + \epsilon)(\tilde{\mathbf{g}}(\theta) + \epsilon - \tilde{\mathbf{g}}(\theta) - \epsilon') \quad (52)$$

$$= \lambda(\tilde{\mathbf{g}}(\theta) + \epsilon)(\epsilon - \epsilon') \quad (53)$$

Note that ϵ and ϵ' are random variables with zero mean ($E(\epsilon) = E(\epsilon') = 0$) and the variance of ϵ is $\sigma^2(\theta)$. They are also independent. Therefore the expectation of ∇ is simplified as:

$$E_{D, D' \sim \mathcal{Z}^n}(\nabla) = E(\lambda \epsilon \cdot \epsilon) + O(\lambda^2) \quad (54)$$

$$= \lambda \sum_j \sigma^2(\theta_j) + O(\lambda^2) \quad (55)$$

where $\sigma^2(\theta_j)$ is the gradient variance of the parameters θ_j . For simplicity, we use σ_j^2 , r_j , and $\mathbf{g}_{D,j}$ to denote $\sigma^2(\theta_j)$, $r(\theta_j)$, and $\mathbf{g}_D(\theta_j)$ respectively.

Next, we denote the empirical generalization gap at t^{th} step as ∇_t , then we have the accumulated generalization gap after training T steps for SB with SGD:

$$\mathbf{GAP}_{SB,SGD} := \nabla_1 + \nabla_2 + \dots + \nabla_T = \sum_{t=1}^T \nabla_t \quad (56)$$

Taking expectation, we have:

$$E(\mathbf{GAP}_{SB,SGD}) = E\left(\sum_{t=1}^T \nabla_t\right) = \sum_{t=1}^T E(\nabla_t) \approx \lambda_0 \sum_{t=1}^T \sum_j \sigma_{t,j}^2 \quad (57)$$

where λ_0 denotes the learning rate of SB. As for LB scenarios, we assume the batch size of LB is k times as the SB, then we have the gradient variance of SB and LB are:

$$\begin{aligned} \sigma_{SB}^2(\theta) &= \text{Var}\left[\frac{1}{B} \sum_{i=1}^B \mathbf{g}_i(\theta)\right] = \frac{1}{B} \rho^2(\theta) \\ \sigma_{LB}^2(\theta) &= \text{Var}\left[\frac{1}{kB} \sum_{i=1}^{kB} \mathbf{g}_i(\theta)\right] = \frac{1}{kB} \rho^2(\theta) \end{aligned} \quad (58)$$

respectively. Similarly, using eq.58, we have the accumulated generalization gap after training T/k steps for LB:

$$E(\mathbf{GAP}_{LB,SGD}) \approx \lambda \sum_{t=1}^{T/k} \sum_j \frac{\sigma_{t,j}^2}{k} \quad (59)$$

If $\sigma_{t,j}$ is t independent, eq.57 and eq.59 are simplified as:

$$E(\mathbf{GAP}_{SB,SGD}) \approx \lambda_0 T \sum_j \sigma_j^2 \quad (60)$$

$$E(\mathbf{GAP}_{LB,SGD}) \approx \frac{\lambda T}{k^2} \sum_j \sigma_j^2 \quad (61)$$

respectively. Taking $\lambda = k^2 \cdot \lambda_0$, $E(\mathbf{GAP}_{LB,SGD})$ will have the same accumulated generalization gap as SB. This is known as the linear/square scaling rules. However, the assumption that " $\sigma_{t,j}$ is t independent" is unrealistic. Similarly, the accumulated generalization gap of VR-SGD in LB scenarios can be written as:

$$E(\mathbf{GAP}_{LB,VR-SGD}) \approx \sum_{t=1}^{T/k} \sum_j \frac{\lambda \cdot r_{t,j} \cdot \sigma_{t,j}^2}{k} = \frac{\lambda}{k} \sum_{t=1}^{T/k} \sum_j \mathbf{g}_{t,j}^2 \quad (62)$$

When training converges, $\mathbf{g}_{t,j} \rightarrow 0$, $\mathbf{g}_{t,j}^2 < \sigma_{t,j}^2$ because $r_{t,j} = \frac{\mathbf{g}_{t,j}^2}{\sigma_{t,j}^2} \rightarrow 0$, which has been verified experimentally (see Figure.4 of [Liu *et al.*, 2020a]). Therefore, we have:

$$\frac{\lambda}{k} \sum_{t=1}^{T/k} \sum_j \mathbf{g}_{t,j}^2 < \lambda \sum_{t=1}^{T/k} \sum_j \frac{\sigma_{t,j}^2}{k} \text{ i.e., } E(\mathbf{GAP}_{LB,VR-SGD}) < E(\mathbf{GAP}_{LB,SGD}) \quad (63)$$

This inequality demonstrates that the generalization ability of VR-SGD is much better than that of SGD.

C Notations

| | |
|--|---|
| \mathcal{Z} | A data distribution satisfies $\mathcal{X} \times \mathcal{Y}$ |
| (x_i, y_i) | A single data sample |
| D | Training set consists of n samples drawn from \mathcal{Z} |
| D' | Test set consists of n' samples drawn from \mathcal{Z} |
| θ | Model parameters, whose components are denoted as θ_j |
| θ^* | The optimal model parameters |
| $\mathbf{g}_i(\theta)$ | Parameters' gradient <i>w.r.t.</i> a single data sample (x_i, y_i) |
| $\tilde{\mathbf{g}}(\theta)$ or $\tilde{\mathbf{g}}_d(\theta)$ | Mean values of parameters' gradient over a total data distribution <i>i.e.</i> , $\mathbb{E}_{s \sim \mathcal{Z}}(\mathbf{g}_i(\theta))$, or gradient over the data on device d . |
| $\mathbf{g}_D(\theta)$ | Average gradient over the training dataset, <i>i.e.</i> , $\frac{1}{n} \sum_{i=1}^n \mathbf{g}_i(\theta)$ |
| $\mathbf{g}_{D'}(\theta)$ | Average gradient over the test dataset, <i>i.e.</i> , $\frac{1}{n'} \sum_{i=1}^{n'} \mathbf{g}'_i(\theta)$. Note that, in eq. (45), we assume $n' = n$ |
| $\rho^2(\theta)$ | Variance of parameters' gradient of a single sample, <i>i.e.</i> , $\text{Var}_{s \sim \mathcal{Z}}(\mathbf{g}_s(\theta))$ |
| $\sigma^2(\theta)$ | Variance of the average gradient over a training dataset of size n , <i>i.e.</i> , $\text{Var}_{D \sim \mathcal{Z}^n}[\mathbf{g}_D(\theta)]$ |
| σ_j^2 | Same as $\sigma^2(\theta_j)$ |
| r_j or $r(\theta_j)$ | Gradient signal to noise ratio (GSNR) of model parameter θ_j |
| $r(\theta_t^{(l)})$ | GSNR of model parameters θ on l^{th} layer at t^{th} step |
| $L[D]$ | Empirical training loss, <i>i.e.</i> , $\frac{1}{n} \sum_{i=1}^n L(y_i, f(x_i, \theta))$ |
| $L[D']$ | Empirical test loss, <i>i.e.</i> , $\frac{1}{n'} \sum_{i=1}^{n'} L(y'_i, f(x'_i, \theta))$ |
| $\Delta L[D]$ | One-step training loss decrease |
| $\Delta L_j[D]$ | One-step training loss decrease caused by updating one parameter θ_j |
| ∇ | One-step generalization gap increment, <i>i.e.</i> , $\Delta L[D] - \Delta L[D']$ |
| $\mathbf{R}(\mathcal{Z}, n)$ | One-step generalization ratio (OSGR) for the training and test sets of size n sampled from data distribution \mathcal{Z} , <i>i.e.</i> , $\frac{\mathbb{E}_{D, D' \sim \mathcal{Z}^n}(\Delta L[D'])}{\mathbb{E}_{D \sim \mathcal{Z}^n}(\Delta L[D])}$ |
| λ | Learning rate |
| G | Upper bound of the gradients <i>w.r.t</i> all training samples |
| σ_l^2 or σ_u^2 | Lower and upper coordinate bounded variance of the gradients |
| r_l or r_u | Lower and upper bound of the GSNR |
| ℓ_i | Upper bound of $\nabla_i^2 L(\theta_t)$ satisfies $u \in \mathcal{R}^d$, $ u^T \nabla_i^2 L(\theta_t) u \leq \ell_i \ u\ ^2$ |
| T | Max training steps |
| ϵ | Random variables with zero mean and variance $\sigma^2(\theta)$ |
| $\mathbf{GAP}_{SB, SGD}$ | Accumulated generalization gap of SGD during small batch scenario |

D Algorithms and Experiments

Algorithm 2: *SGD*

Input: $B = \text{GlobalBatchSize}/\text{DeviceNumber}(k)$

```

1 while  $\theta_t$  not converged do
    for device  $d = 1$  to  $k$  do
         $\tilde{\mathbf{g}}_d(\theta_t) \leftarrow \frac{1}{B} \sum_{i=1}^B \nabla_{\theta} L(y_i, f(x_i, \theta_{t-1}))$  (Get gradient on each GPU/TPU)
     $\tilde{\mathbf{g}}(\theta_t) \leftarrow \frac{1}{k} \sum_{d=1}^k \tilde{\mathbf{g}}_d(\theta_t)$  (Reduce gradient over all devices)
     $\theta_t \leftarrow \theta_{t-1} - \lambda \cdot \tilde{\mathbf{g}}(\theta_t)$  (Update weights)

```

Algorithm 3: *VR – Adam*

Input: require device number $k \geq 2$

Input: $B = \text{GlobalBatchSize}/k$

Input: $\gamma_1 = 0.1$

Input: $\beta_1, \beta_2 \in [0, 1)$ (1^{st} and 2^{nd} order decay rates for momentum of gradient)

Input: $\beta_3 \in [0, 1)$ (1^{st} order decay rates for momentum of GSNR)

```

1 while  $\theta_t$  not converged do
     $m_0 \leftarrow 0$  (Initialize  $1^{st}$  order momentum of gradient)
     $v_0 \leftarrow 0$  (Initialize  $2^{nd}$  order momentum of gradient)
     $p_0 \leftarrow 0$  (Initialize  $1^{st}$  order momentum of GSNR)
     $t \leftarrow 0$  (Initialize train step)
    for device  $d = 1$  to  $k$  do
         $\tilde{\mathbf{g}}_d(\theta_t) \leftarrow \frac{1}{B} \sum_{i=1}^B \nabla_{\theta} L(y_i, f(x_i, \theta_{t-1}))$  (Get gradient on each GPU/TPU)
         $\tilde{\mathbf{g}}_d^2(\theta_t) \leftarrow \tilde{\mathbf{g}}_d(\theta_t) \otimes \tilde{\mathbf{g}}_d(\theta_t)$  (Element-wise multiply, so as square terms below)
     $\tilde{\mathbf{g}}(\theta_t) \leftarrow \frac{1}{k} \sum_{d=1}^k \tilde{\mathbf{g}}_d(\theta_t)$  (Reduce gradient over all devices)
     $\sigma_t^2 \leftarrow \frac{1}{k} \sum_{d=1}^k \tilde{\mathbf{g}}_d^2(\theta_t) - \tilde{\mathbf{g}}^2(\theta_t)$  (Compute gradient variance)
     $r(\theta_t) \leftarrow \frac{\tilde{\mathbf{g}}^2(\theta_t)}{\sigma_t^2}$  (Compute GSNR)
    for layer  $l = 0$  to  $m$  do
         $r(\theta_t^{(l)}) \leftarrow \frac{r(\theta_t^{(l)})}{\frac{1}{J} \sum_{j=1}^J r(\theta_{t,j}^{(l)})}$  (Normalize GSNR so that  $\overline{r(\theta_t^{(l)})} = 1$ )
         $r(\theta_t^{(l)}) \leftarrow \begin{cases} \gamma_1 & \text{if } r(\theta_t^{(l)}) < \gamma_1 \\ 1 & \text{if } r(\theta_t^{(l)}) > 1 \end{cases}$  (Confine the max/min ratio within  $\frac{1}{\gamma_1}$ )
     $p_t \leftarrow \beta_3 \cdot p_{t-1} + (1 - \beta_3) \cdot r(\theta_t)$  (Update  $1^{st}$  order biased momentum of GSNR)
     $\hat{p}_t \leftarrow p_t / (1 - \beta_3^t)$  (Bias correction)
     $\hat{\mathbf{g}}(\theta_t) \leftarrow \hat{p}_t \cdot \tilde{\mathbf{g}}(\theta_t)$  (Adapt gradient mean with GSNR)
     $m_t \leftarrow \beta_1 \cdot m_{t-1} + (1 - \beta_1) \cdot \hat{\mathbf{g}}(\theta_t)$  (Update  $1^{st}$  order biased momentum)
     $v_t \leftarrow \beta_2 \cdot v_{t-1} + (1 - \beta_2) \cdot \hat{\mathbf{g}}^2(\theta_t)$  (Update  $2^{nd}$  order biased momentum)
     $\hat{m}_t \leftarrow m_t / (1 - \beta_1^t)$  (Bias correction)
     $\hat{v}_t \leftarrow v_t / (1 - \beta_2^t)$  (Bias correction)
     $\theta_t \leftarrow \theta_{t-1} - \lambda \cdot \hat{m}_t / (\sqrt{\hat{v}_t} + \varepsilon)$  (Update weights)

```

Algorithm 4: Adam

Input: $\beta_1, \beta_2 \in [0, 1)$ (1^{st} and 2^{nd} order decay rates for momentum)

```
1 while  $\theta_t$  not converged do
     $m_0 \leftarrow 0$  (Initialize  $1^{st}$  order momentum of gradient)
     $v_0 \leftarrow 0$  (Initialize  $2^{nd}$  order momentum of gradient)
     $t \leftarrow 0$  (Initialize train step)
    for device  $d = 1$  to  $k$  do
         $\tilde{\mathbf{g}}_d(\theta_t) \leftarrow \frac{1}{B} \sum_{i=1}^B \nabla_{\theta} L(y_i, f(x_i, \theta_{t-1}))$  (Get gradient on each GPU/TPU)
     $\tilde{\mathbf{g}}(\theta_t) \leftarrow \frac{1}{k} \sum_{d=1}^k \tilde{\mathbf{g}}_d(\theta_t)$  (Reduce gradient over all devices)
     $m_t \leftarrow \beta_1 \cdot m_{t-1} + (1 - \beta_1) \cdot \tilde{\mathbf{g}}(\theta_t)$  (Update  $1^{st}$  order biased momentum of gradient)
     $v_t \leftarrow \beta_2 \cdot v_{t-1} + (1 - \beta_2) \cdot \tilde{\mathbf{g}}^2(\theta_t)$  (Update  $2^{nd}$  order biased momentum of gradient)
     $\hat{m}_t \leftarrow m_t / (1 - \beta_1^t)$  (Bias correction)
     $\hat{v}_t \leftarrow v_t / (1 - \beta_2^t)$  (Bias correction)
     $\theta_t \leftarrow \theta_{t-1} - \lambda \cdot \hat{m}_t / (\sqrt{\hat{v}_t} + \varepsilon)$  (Update weights)
```

Algorithm 5: VR – LAMB

Input: require device number $k \geq 2$

Input: $B = \text{GlobalBatchSize}/k$

Input: $\gamma_1 = 0.1$

Input: $\beta_1, \beta_2 \in [0, 1)$ (1^{st} and 2^{nd} order decay rates for momentum)

Input: $\beta_3 \in [0, 1)$ (1^{st} order decay rates for momentum of GSNR)

```
1 while  $\theta_t$  not converged do
     $m_0 \leftarrow 0$  (Initialize  $1^{st}$  order momentum of gradient)
     $v_0 \leftarrow 0$  (Initialize  $2^{nd}$  order momentum of gradient)
     $p_0 \leftarrow 0$  (Initialize  $1^{st}$  order momentum of GSNR)
     $t \leftarrow 0$  (Initialize train step)
    for device  $d = 1$  to  $k$  do
         $\tilde{\mathbf{g}}_d(\theta_t) \leftarrow \frac{1}{B} \sum_{i=1}^B \nabla_{\theta} L(y_i, f(x_i, \theta_{t-1}))$  (Get gradient on each GPU/TPU)
         $\tilde{\mathbf{g}}_d^2(\theta_t) \leftarrow \tilde{\mathbf{g}}_d(\theta_t) \otimes \tilde{\mathbf{g}}_d(\theta_t)$  (Element-wise multiply, so as square terms below)
     $\tilde{\mathbf{g}}(\theta_t) \leftarrow \frac{1}{k} \sum_{d=1}^k \tilde{\mathbf{g}}_d(\theta_t)$  (Reduce gradient over all devices)
     $\sigma_t^2 \leftarrow \frac{1}{k} \sum_{d=1}^k \tilde{\mathbf{g}}_d^2(\theta_t) - \tilde{\mathbf{g}}^2(\theta_t)$  (Compute gradient variance)
     $r(\theta_t) \leftarrow \frac{\tilde{\mathbf{g}}^2(\theta_t)}{\sigma_t^2}$  (Compute GSNR)
    for layer  $l = 0$  to  $m$  do
         $r(\theta_t^{(l)}) \leftarrow \frac{r(\theta_t^{(l)})}{\frac{1}{J} \sum_{j=1}^J r(\theta_{t,j}^{(l)})}$  (Normalize GSNR so that  $\overline{r(\theta_t^{(l)})} = 1$ )
         $r(\theta_t^{(l)}) \leftarrow \begin{cases} \gamma_1 & \text{if } r(\theta_t^{(l)}) < \gamma_1 \\ 1 & \text{if } r(\theta_t^{(l)}) > 1 \end{cases}$  (Confine the max/min ratio within  $\frac{1}{\gamma_1}$ )
     $p_t \leftarrow \beta_3 \cdot p_{t-1} + (1 - \beta_3) \cdot r(\theta_t)$  (Update  $1^{st}$  order biased momentum of GSNR)
     $\hat{p}_t \leftarrow p_t / (1 - \beta_3^t)$  (Bias correction)
     $\hat{\mathbf{g}}(\theta_t) \leftarrow \hat{p}_t \cdot \tilde{\mathbf{g}}(\theta_t)$  (Adapt gradient mean with GSNR)
     $m_t \leftarrow \beta_1 \cdot m_{t-1} + (1 - \beta_1) \cdot \hat{\mathbf{g}}(\theta_t)$  (Update  $1^{st}$  order biased momentum)
     $v_t \leftarrow \beta_2 \cdot v_{t-1} + (1 - \beta_2) \cdot \tilde{\mathbf{g}}^2(\theta_t)$  (Update  $2^{nd}$  order biased momentum)
     $\hat{m}_t \leftarrow m_t / (1 - \beta_1^t)$  (Bias correction)
     $\hat{v}_t \leftarrow v_t / (1 - \beta_2^t)$  (Bias correction)
     $\hat{\mathbf{G}}(\theta_t) \leftarrow \hat{m}_t / (\sqrt{\hat{v}_t} + \varepsilon)$ 
    for layer  $l = 0$  to  $m$  do
         $\theta_t^{(l)} \leftarrow \theta_{t-1}^{(l)} - \lambda \cdot \frac{\phi(\|\theta_t^{(l)}\|)}{\|\hat{\mathbf{G}}(\theta_t)\|} \cdot \hat{\mathbf{G}}(\theta_t)$  (Update weights)
```

Algorithm 6: LAMB**Input:** $\beta_1, \beta_2 \in [0, 1]$ (1^{st} and 2^{nd} order decay rates for momentum)**Input:** scaling function ϕ **1 while** θ_t not converged **do** $m_0 \leftarrow 0$ (Initialize 1^{st} order momentum of gradient) $v_0 \leftarrow 0$ (Initialize 2^{nd} order momentum of gradient) $t \leftarrow 0$ (Initialize train step) **for device** $d = 1$ **to** k **do** $\tilde{\mathbf{g}}_d(\theta_t) \leftarrow \frac{1}{B} \sum_{i=1}^B \nabla_{\theta} L(y_i, f(x_i, \theta_{t-1}))$ (Get gradient on each GPU/TPU) $\tilde{\mathbf{g}}(\theta_t) \leftarrow \frac{1}{k} \sum_{d=1}^k \tilde{\mathbf{g}}_d(\theta_t)$ (Reduce gradient over all devices) $m_t \leftarrow \beta_1 \cdot m_{t-1} + (1 - \beta_1) \cdot \tilde{\mathbf{g}}(\theta_t)$ (Update 1^{st} order biased momentum) $v_t \leftarrow \beta_2 \cdot v_{t-1} + (1 - \beta_2) \cdot \tilde{\mathbf{g}}^2(\theta_t)$ (Update 2^{nd} order biased momentum) $\hat{m}_t \leftarrow m_t / (1 - \beta_1^t)$ (Bias correction) $\hat{v}_t \leftarrow v_t / (1 - \beta_2^t)$ (Bias correction) $\hat{\mathbf{g}}(\theta_t) \leftarrow \hat{m}_t / (\sqrt{\hat{v}_t} + \varepsilon)$ **for layer** $l = 0$ **to** m **do** $\theta_t^{(l)} \leftarrow \theta_{t-1}^{(l)} - \lambda \cdot \frac{\phi(\|\theta_t^{(l)}\|)}{\|\hat{\mathbf{g}}(\theta_t)\|} \cdot \hat{\mathbf{g}}(\theta_t)$ (Update weights)Table 9: Hyper-parameters of **BERT pretraining** with VR-LAMB.

| Batch Size | Steps | Warm-up Steps | Phase-1 LR | Phase-1 Acc-steps (k) | Warm-up Steps | Phase-2 LR | Phase-2 Acc-steps (k) | F1 Score |
|------------|-------|---------------|------------|-----------------------|---------------|------------|-----------------------|----------|
| 16k | 31250 | 2800 | 0.0035 | 8 | 280 | 0.0035 | 32 | 91.42 |
| 32k | 15625 | 2800 | 0.0053 | 8 | 280 | 0.0053 | 32 | 91.58 |
| 64k/32k | 8599 | 2000 | 0.007 | 8 | 200 | 0.0045 | 32 | 91.49 |
| 64k | 7820 | 2000 | 0.007 | 8 | 200 | 0.0055 | 64 | 91.30 |
| 96k/32k | 6256 | 1870 | 0.007 | 12 | 200 | 0.00575 | 32 | 91.23 |
| 96k | 5214 | 1870 | 0.007 | 12 | 187 | 0.0055 | 96 | 90.70 |
| 128k/64k | 4301 | 1760 | 0.007 | 16 | 200 | 0.00575 | 64 | 90.85 |

Note that $\gamma = 0.1$ for all batch size. Acc-steps in NVIDIA's code is equivalent to device number k .Table 10: Hyper-parameters of **ImageNet** trained with VR-LARS optimizer on ResNet50.

| Batch Size | Warm-up Epochs | Best LR | Device Number (k) | Test Accuracy |
|------------|----------------|-------------------|-------------------|---------------|
| 2k | 0.625 | $7 \cdot 2^0$ | 8 | 77.14% |
| 4k | 1.25 | $7 \cdot 2^{0.5}$ | 8 | 77.23% |
| 8k | 2.5 | $7 \cdot 2^1$ | 16 | 77.36% |
| 16k | 5 | $7 \cdot 2^{1.5}$ | 32 | 77.27% |
| 32k | 14 | $7 \cdot 2^2$ | 64 | 76.81% |
| 64k | 40 | 37 | 128 | 75.86% |
| 96k | 41 | 38 | 192 | 74.82% |

Note that $\gamma = 0.1$ for all batch size.Table 11: Hyper-parameters of **DLRM** trained with SGD and VR-SGD.

| Opt | Batch Size | Warm-up Epochs | LR | Test Accuracy | Opt | Batch Size | Warm-up Epochs | LR | Test Accuracy |
|-----|------------|----------------|-----------|---------------|--------|------------|----------------|-----------|---------------|
| SGD | 32k | $1/2^4$ | $2^{3.5}$ | 0.8014 | VR-SGD | 32k | $1/2^4$ | $2^{3.5}$ | 0.8026 |
| | 64k | $1/2^3$ | 2^4 | 0.8025 | | 64k | $1/2^3$ | 2^4 | 0.8048 |
| | 128k | $1/2^2$ | $2^{4.5}$ | 0.8021 | | 128k | $1/2^2$ | $2^{4.5}$ | 0.8042 |
| | 256k | $1/2$ | 2^5 | 0.7827 | | 256k | $1/2$ | 2^5 | 0.8023 |
| | 512k | $3/4$ | $2^{5.5}$ | 0.7787 | | 512k | $3/4$ | $2^{5.5}$ | 0.8013 |

Note that $\gamma = 0.1$ and device number $k = 8$ for all batch size.

Table 12: Hyper-parameters of **CIFAR10** trained with Momentum/Adam/LAMB/LARS optimizers and their corresponding VRGD optimizers.

| Opt | Batch Size | Warm-up Epochs | LR | Test Accuracy | Opt | Batch Size | Warm-up Epochs | LR | Test Accuracy |
|----------|------------|----------------|-----------------------------------|---------------|-------------|------------|----------------|-----------------------------------|---------------|
| Momentum | 256 | 2^2 | $\frac{128}{2^2 \times 100}$ | 93.68% | VR-Momentum | 256 | 2^2 | $\frac{128}{2^2 \times 100}$ | 93.79% |
| | 512 | $2^{2.5}$ | $\frac{128}{2^{1.5} \times 100}$ | 93.56% | | 512 | $2^{2.5}$ | $\frac{128}{2^{1.5} \times 100}$ | 93.71% |
| | 1k | 2^3 | $\frac{128}{2^1 \times 100}$ | 93.17% | | 1k | 2^3 | $\frac{128}{2^1 \times 100}$ | 93.50% |
| | 2k | $2^{3.5}$ | $\frac{128}{2^{0.5} \times 100}$ | 92.19% | | 2k | $2^{3.5}$ | $\frac{128}{2^{0.5} \times 100}$ | 93.28% |
| | 4k | 2^4 | $\frac{128}{2^0 \times 100}$ | 17.40% | | 4k | 2^4 | $\frac{128}{2^0 \times 100}$ | 92.70% |
| | 8k | 2^5 | $\frac{128}{2^{-0.5} \times 100}$ | 14.57% | | 8k | 2^5 | $\frac{128}{2^{-0.5} \times 100}$ | 90.57% |
| Adam | 256 | 2^2 | $\frac{192}{2^3 \times 1e4}$ | 91.88% | VR-Adam | 256 | 2^2 | $\frac{192}{2^3 \times 1e4}$ | 92.46% |
| | 512 | $2^{2.5}$ | $\frac{192}{2^{2.5} \times 1e4}$ | 92.24% | | 512 | $2^{2.5}$ | $\frac{192}{2^{2.5} \times 1e4}$ | 92.40% |
| | 1k | 2^3 | $\frac{192}{2^2 \times 1e4}$ | 92.02% | | 1k | 2^3 | $\frac{192}{2^2 \times 1e4}$ | 92.43% |
| | 2k | $2^{3.5}$ | $\frac{192}{2^1 \times 1e4}$ | 91.98% | | 2k | $2^{3.5}$ | $\frac{192}{2^1 \times 1e4}$ | 92.10% |
| | 4k | 2^4 | $\frac{192}{2^0 \times 1e4}$ | 59.38% | | 4k | 2^4 | $\frac{192}{2^0 \times 1e4}$ | 91.74% |
| | 8k | 2^5 | $\frac{192}{2^{-1} \times 1e4}$ | 20.74% | | 8k | 2^5 | $\frac{192}{2^{-1} \times 1e4}$ | 90.86% |
| LAMB | 256 | 2^2 | $\frac{64}{2^4 \times 1e3}$ | 92.08% | VR-LAMB | 256 | 2^2 | $\frac{64}{2^4 \times 1e3}$ | 92.29% |
| | 512 | $2^{2.5}$ | $\frac{64}{2^{3.5} \times 1e3}$ | 92.03% | | 512 | $2^{2.5}$ | $\frac{64}{2^{3.5} \times 1e3}$ | 92.34% |
| | 1k | 2^3 | $\frac{64}{2^3 \times 1e3}$ | 91.90% | | 1k | 2^3 | $\frac{64}{2^3 \times 1e3}$ | 92.05% |
| | 2k | $2^{3.5}$ | $\frac{64}{2^2 \times 1e3}$ | 92.13% | | 2k | $2^{3.5}$ | $\frac{64}{2^2 \times 1e3}$ | 92.43% |
| | 4k | 2^4 | $\frac{64}{2^1 \times 1e3}$ | 58.35% | | 4k | 2^4 | $\frac{64}{2^1 \times 1e3}$ | 92.04% |
| | 8k | 2^5 | $\frac{64}{2^1 \times 1e3}$ | 15.13% | | 8k | 2^5 | $\frac{64}{2^1 \times 1e3}$ | 91.07% |
| LARS | 256 | 2^2 | $\frac{896}{2^2 \times 100}$ | 92.30% | VR-LARS | 256 | 2^2 | $\frac{896}{2^2 \times 100}$ | 92.35% |
| | 512 | $2^{2.5}$ | $\frac{896}{2^{1.5} \times 100}$ | 92.29% | | 512 | $2^{2.5}$ | $\frac{896}{2^{1.5} \times 100}$ | 92.53% |
| | 1k | 2^3 | $\frac{896}{2^1 \times 100}$ | 92.34% | | 1k | 2^3 | $\frac{896}{2^1 \times 100}$ | 92.44% |
| | 2k | $2^{3.5}$ | $\frac{896}{2^{0.5} \times 100}$ | 82.39% | | 2k | $2^{3.5}$ | $\frac{896}{2^{0.5} \times 100}$ | 92.79% |
| | 4k | 2^4 | $\frac{896}{2^0 \times 100}$ | 27.50% | | 4k | 2^4 | $\frac{896}{2^0 \times 100}$ | 92.35% |
| | 8k | 2^5 | $\frac{896}{2^{-0.5} \times 100}$ | 12.21% | | 8k | 2^5 | $\frac{896}{2^{-0.5} \times 100}$ | 91.86% |

Note that $\gamma = 0.1$ and device number $k = 8$ for all batch size.

Table 13: Learning rate of VR-LARS comparing with LARS on **ImageNet**.

| Batch Size | LARS | VR-LARS(ours) |
|------------|------|-------------------|
| 2k | - | $7 \cdot 2^0$ |
| 4k | - | $7 \cdot 2^{0.5}$ |
| 8k | - | $7 \cdot 2^1$ |
| 16k | - | $7 \cdot 2^{1.5}$ |
| 32k | 35 | $7 \cdot 2^2$ |
| 64k | 41 | 37 |
| 96k | 43 | 38 |

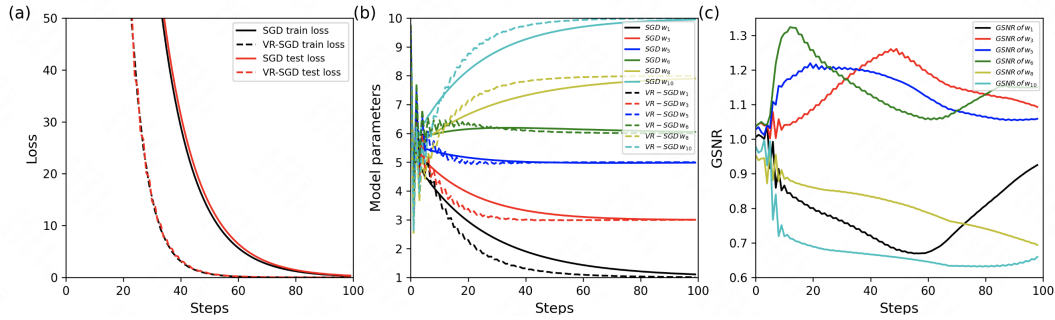


Figure 5: **Linear Regression** experiments trained with SGD and VR-SGD: (a) training and test loss (batch size = 256); (b) model parameters $w_i, i \in [1, 10]$; (c) GSNR of model parameters before max/min constraint used in VR-SGD. Note that $w_i, i \in (2, 4, 7, 9)$ are omitted for simplicity. They behave almost the same as their neighbors.

E Wall Clock Time

Table.14 and Table.15 show the wall clock time using VR-LAMB and VR-LARS respectively. Results indicate that training BERT with 128k/64k batch size and using 768 GPUs (A100), we can achieve the desired F1 score within 64.1m. Similarly, training ImageNet with 96k batch size and 192 GPUs just costs 18.9m.

Table 14: Training time of **BERT pretraining**.

| Batch Size | 16k | 32k | 64k | 96k | 128k/64k |
|------------|--------|--------|--------|-------|----------|
| GPUs | 96 | 192 | 384 | 576 | 768 |
| VR-LAMB | 367.4m | 204.1m | 113.4m | 79.8m | 64.1m |

Table 15: Training time of **ImageNet** using ResNet50.

| Batch Size | 2k | 4k | 8k | 16k | 32k | 64k | 96k |
|------------|--------|--------|--------|-------|-------|-------|-------|
| GPUs | 4 | 8 | 16 | 32 | 64 | 128 | 192 |
| VR-LARS | 480.1m | 266.7m | 148.2m | 82.3m | 45.7m | 25.4m | 18.9m |